STRUCTURAL EVALUATION

OF FIXED OFFSHORE PLATFORMS

by

J. KIM VANDIVER

B.S., Harvey Mudd College
(1968)

S.M., Massachusetts Institute of Technology
(1969)

SUBMITTED IN PARTIAL FULFILLMENT OF THE
REQUIREMENTS FOR THE DEGREE OF
DOCTOR OF PHILOSOPHY

at the

MASSACHUSETTS INSTITUTE OF TECHNOLOGY

and the

WOODS HOLE OCEANOGRAPHIC INSTITUTION

January, 1975

Signature of Author.....
Joint Program in Ocean Engineering, Massachusetts Institute of Technology - Woods Hole Oceanographic Institution, and Department of Ocean Engineering, Massachusetts Institute of Technology, January, 1975

Certified by.....
Thesis Supervisor

Accepted by.....
Chairman, Joint Committee on Ocean Engineering, Massachusetts Institute of Technology - Woods Hole Oceanographic Institution

STRUCTURAL EVALUATION OF FIXED OFFSHORE PLATFORMS

by J. Kim Vandiver

ABSTRACT

In fixed offshore structures, damage incurred below the waterline is often difficult to detect, but significant enough to be the source of a subsequent massive failure. A technique is described that can be used to detect subsurface structural failure by detecting changes in the natural frequencies of the structure. One tower was extensively studied; the dynamic measurement and analysis techniques are described. A parallel computer model of this tower was used to simulate the effect of removal of structural members on natural frequency. The parameters which determine the level of minimum detectable damage are discussed.

Experimental data correlating wind and wave height spectra to observed structure response is presented. Statistical Energy Analysis is introduced as a method for predicting the dynamic response of offshore towers to random waves. The method is superior to the classical random vibration approach, in that it does not require the calculation of the wave force spectrum from the wave height spectrum, thus eliminating the calculations and assumptions common to the frequently used Morrison wave force equation. SEA is also applicable to a broad range of fixed and floating structures.

ACKNOWLEDGEMENTS

This research was sponsored by the American Bureau of Shipping and by the Massachusetts Institute of Technology - Woods Hole Oceanographic Institution Joint Program in Ocean Engineering.

The advice and encouragement of many people were essential to the completion of this work. Particular credit must be given to my thesis advisor J. Harvey Evans and the members of my thesis committee: Professors R.H. Lyon, A.E. Mansour and E.H. Vanmarcke of M.I.T., and Mr. J.W. Mavor of W.H.O.I.

The generous cooperation and support of many U.S. Coast Guard and Boston Naval Shipyard personnel was vital to the success of the experimental program.

My wife, Pam, made numerous contributions along the way, as well as the typing when the need arose.

TABLE OF CONTENTS

TABLE OF CONTENTS, CONTINUED

LIST OF FIGURES

LIST OF TABLES

LIST OF SYMBOLS

x, y, z	Displacement coordinates
$x, \dot{x}, y, \dot{y}$	x and y velocity and acceleration
$\theta, \dot{\theta}, \ddot{\theta}$	Angular displacement, velocity and acceleration
y_{max}	y coordinate of an accelerometer
f	Frequency in Hertz
f_o	Natural frequency of single d.o.f. system
$\Delta f_e, \Delta f$	Equivalent bandwidth , half power bandwidth
ω	Frequency in radians/second
ω_o	Natural frequency of single d.o.f. system
$\omega_x, \omega_y, \omega_\theta$	Natural frequencies of the tower in x, y, and θ modes
K	Spring constant in pounds/ft
K_1, K_2, K_3	Spring constant in x, y, and θ modes
$[K]$	Stiffness matrix
M	Mass in slugs of single d.o.f. resonator
$[M]$	Mass matrix
$\{x\}$	Eigenvector in multi-d.o.f. system
J	Moment of inertia in slug-ft^2
ζ	Damping ratio
R	Mechanical resistance
R_3	Mechanical resistance in torsion
$F(t), T(t)$	Driving force or torque on a resonator

LIST OF SYMBOLS, CONTINUED

$X(\omega)$	Fourier transform of response $x(t)$
$H(\omega)$	Fourier transform of response $x(t)$ to a unit impulse $\delta(t)$
$F(\omega)$	Fourier transform of force $F(t)$
$E[F^2]$	Mean square of $F(t)$
$S_x(\omega)$, $S_{\dot{x}}(\omega)$, $S_{\ddot{x}}(\omega)$	Displacement, velocity and acceleration response spectra
$E[x^2]$, $E[\dot{x}^2]$, $E[\ddot{x}^2]$	Mean square displacement, velocity and acceleration
$S_F(\omega)$	Single sided power spectrum of force $F(t)$ in lb^2-sec
S_o	White noise force spectrum
$S_p(f)$, $S_v(f)$, $S_F(f)$	Single sided wind pressure, velocity and force spectra
V_1, P_1	Maximum mean wind speed, and pressure at top of tower
ρ	Air or water density as appropriate
C_p	Pressure coefficient
J_z^2, J_H^2	Size reduction factors
C_T	Terrain roughness coefficient
V_{33}	Mean wind speed 33 feet above the surface
A	Cross-sectional area of tower
$\eta(x,t)$	Equation of free surface
E	Average energy per unit area for a regular wave
$E(\omega)$	Energy density per unit area in a random sea
g	Acceleration of gravity
$S_\eta(\omega)$	Wave height spectrum

LIST OF SYMBOLS, CONTINUED

ℓ_1, ℓ_2	Dimensions of a rectangular ocean
k_1, k_2	Seiche wave numbers in rectangular ocean
K	Mode wave number
ϕ	Velocity potential or phase angle as appropriate
$n(\omega)$, $n(k)$	Modal density in frequency and wave number
C_g, C_ϕ	Group and phase velocity
$\langle E \rangle_{mode}$	Average energy per mode in ocean
$\langle E_j \rangle$	Average energy of a resonator in jth mode
R_r, R_i	Radiation and internal damping coefficients
F	Wave forces on a fixed body: the blocked force
Ω	Incidence angle
$\Gamma(\omega,\Omega)$	Shape function

I. INTRODUCTION

As offshore platforms are erected in progressively deeper waters, the problem of on site inspection of subsurface structural members becomes increasingly difficult and expensive. The current use of divers is hampered by poor visibility, poor lighting and hazardous conditions. These obstacles worsen rapidly with increase in depth. In addition, marine growth and corrosion may conceal structural defects.

The inadequacy of current inspection techniques is amplified by the surprizing number of total or near total loss of platforms already in service[1]. Many of these losses may have been preceded by less severe subsurface structural failure that went undetected, and eventually became the source of widespread failure. Had inspection techniques been available to detect these minor changes, the total losses might have been avoided. Among these initially minor sources of failure must be included scouring and progressive failure of bottom conditions, and corrosion of structural members.

The inspection technique described here requires periodic measurement of selected natural frequencies that show direct response to wind and waves. Wind and wave force spectra are sufficiently broad band random excitation to drive most offshore structures at one or more of their natural frequencies. Accelerometers can be used to measure the platform response, and from the records the natural frequencies can be determined.

Such determinations might be made on a semiannual or annual basis. A detected shift in natural frequency between successive measurements would indicate a change in the mass or stiffness of the structure. A reduction in stiffness implies failure in the structural members and joints, or in the supporting bottom conditions. In some circumstances the measurements might be helpful in determining the location of the failure. At the very least the periodic inspection can be used as the "go" or "no go" decision maker for a much more expensive diver survey.

The minimum detectable level of damage that can be determined by this technique will be a measure of its usefullness as an inspection tool. For this to be a valid inspection method for a given type of offshore structure there must exist a broad range of detectable structural failures that lie between the level of minimum detection and obvious failure. In other words, the detection threshold of the technique must be sufficiently sensitive to allow time for repairs to be made before obvious failure occurs.

A detailed study of one offshore pile supported tower was conducted, and the detection threshold was determined. The tower is a welded steel space frame with four primary legs, braced with horizontal and diagonal members. It is fixed to driven steel piles and stands 150 feet above the mudline in 70 feet of water and weighs approximately 600 tons. The tower serves as a manned United States Coast Guard Light Station near the Massachusetts coast. Though small by most standards, its

limited size made an in depth survey possible. Figure I -1.

To determine the detection threshold it is necessary to compare the accuracy of on site frequency measurements to the amount of change caused by a particular structural failure. As it was impossible to arrange a systematic survey of a full scale platform with a variety of before and after structural failures, then the best substitute was a computer simulation of the structure in which the change in stiffness due to a prescribed structural failure could be evaluated. From the stiffness the shift in predicted natural frequency could be determined.

A careful computer simulation of the Buzzards Bay Light Station was prepared using the M.I.T. ICES-STRUDL II[2] structures program. A systematic study of the effect of structural damage was conducted and the results compared to the accuracy of experimental determinations of natural frequency. It was found that except for a few of the most insignificant members, the determination of natural frequency was accurate enough to detect failure of individual subsurface members. In some circumstances it would even be possible to isolate the general location of the break. It was also determined that widespread corrosior would cause a detectable change.

The experimental techniques, computer simulation, and excitation response data for the Buzzards Bay Light Station are presented in detail in the remainder of this paper. Part One of this thesis addresses the detection of subsurface structural

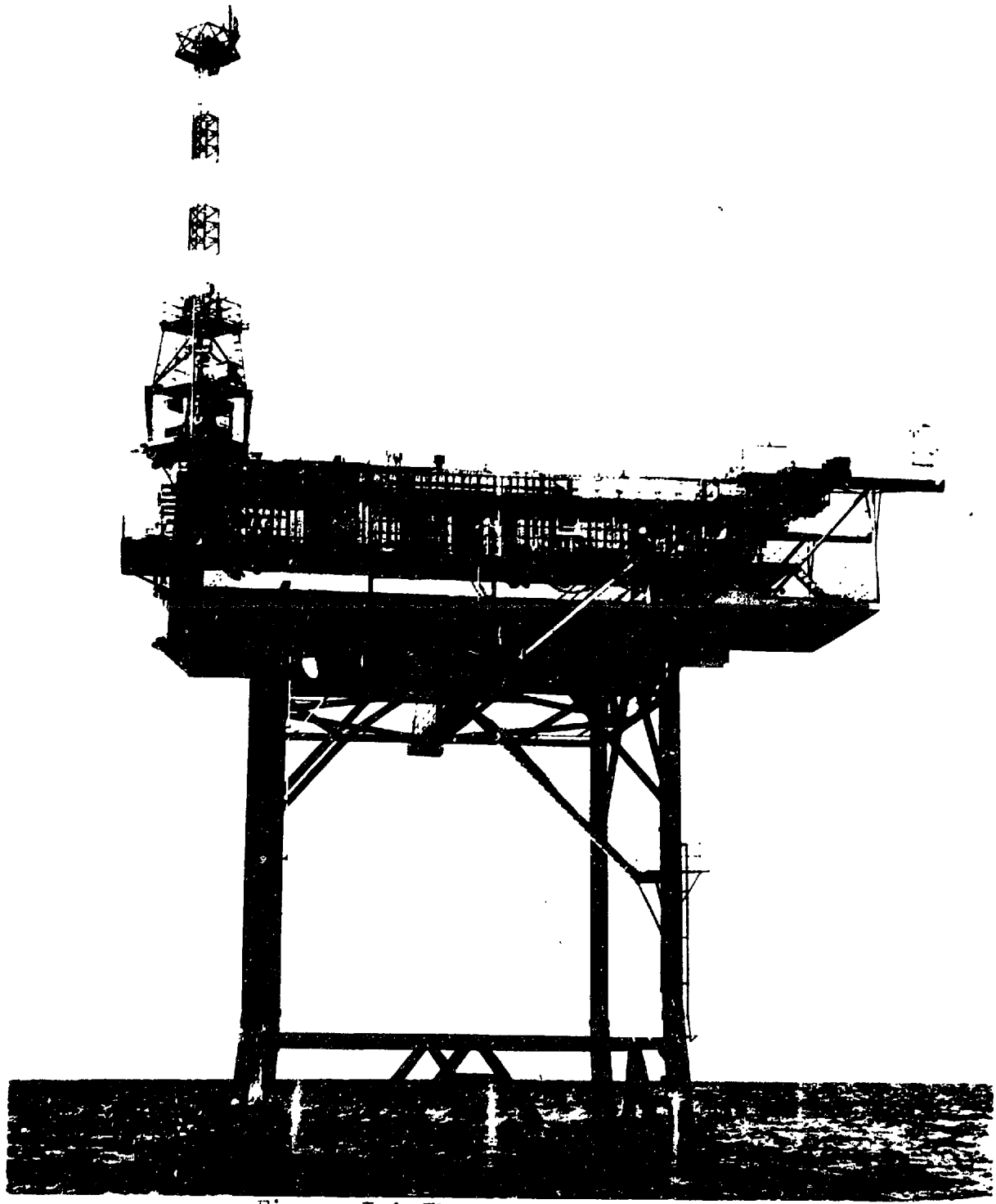

Figure I-1 The Buzzards Bay Tower

failure by measured changes in natural frequency. As discussed above, the instrumentation, computer simulation, estimation of structural mass, and determination of the detection threshold are all presented in detail.

The analysis of the excitation response relations for an offshore structure is quite a different subject from the detection of subsurface failure of individual members. Though it may appear unusual that a doctoral dissertation be composed of two rather distinct problems, it was the outcome of a logical sequence of events. The committee, which examined the original thesis proposal covering the detection of subsurface failure, felt that an adequate treatment of the subject would require at the very least a good understanding of the mechanisms by which wind and wave forces excited structural response.

In the course of satisfying this requirement it became apparent that an important analytic contribution might be made using Statistical Energy Analysis to predict structural response to wave excitation. This method had been applied in other fields, notably acoustics, but its application to an ocean engineering problem had not as yet been published. This was an attractive opportunity, and though it represents an addition to the original thesis proposal, it is hoped that this addition will prove to be a significant contribution to the field.

Part Two considers the dynamic response of offshore structures to random wind and wave forces. Current practice in estimating dynamic response to random wave forces employs the Morrison wave force equation to estimate the force on the structure due to a sinusoidal wave and then generalizes the results to include a random wave height spectra such as the Pierson-Moskowitz. Using classical random vibration theory, this calculated wave force spectra is then used to calculate the response of the structure.

Statistical Energy Analysis (SEA) is introduced as a method for calculating dynamic response due to random waves. This technique eliminates the explicit calculation of wave forces and is consequently substantially easier to use. The dynamic response to wind and waves is predicted for the Buzzards Bay Entrance Tower. This prediction is compared to the response data which was recorded over a broad range of wind and sea state conditions with excellent agreement between measured and predicted response. The response to wind forces is calculated using currently accepted techniques.

A derivation of SEA techniques for offshore structural problems is presented, and it is shown that SEA is applicable to many offshore structural problems, including floating as well as fixed structures.

PART ONE:
DETECTION OF STRUCTURAL FAILURE BY MEASURED
CHANGES IN NATURAL FREQUENCY

II. INTRODUCTION AND STATE OF THE ART

A. Introduction

Before dawn 6 May 1974 a vessel displacing approximately 900 tons struck the Buzzards Bay Entrance Tower, which weighs about 600 tons. One crew member on the tower was thrown from his bunk by the impact. After dawn a visual inspection revealed no above water line damage. Most of the supporting jacket is hidden below the water line, and its condition was unknown.

Fortunately, the natural frequencies of this tower in flexure and rotation had been previously determined. By noon a United States Coast Guard helicopter had transported the author and the necessary measurement equipment to the tower. By 1800 hours it was determined that no significant damage had been incurred below the water line. Ultrasonics tests conducted by divers in August 1974 confirmed these findings. The following sections discuss the testing techniques that were employed and presents the appropriate background theory.

B. State of the Art

The detection of structural failure by measuring a related change in natural frequency is not without precedent. There is continuing industrial research in the field of expensive rotating machinery such as generators and jet engines. More closely related work has been done by civil engineers interested in

the seismic response properties of large buildings. For several years civil engineers have been able to measure the natural frequencies of large buildings using sensitive accelerometers. Wind and seismic forces are sufficiently broad band random excitation that most buildings respond at one or more natural frequencies that are included in the band. Measurements that have been made before and after earthquakes have revealed damage related frequency reductions as large as 50% (3). In many cases visual inspection had revealed no damage. For example, in steel reinforced concrete buildings, microcracks developed in the concrete that went undetected in visual inspections, and yet caused a substantial reduction in the structural stiffness, and therefore, the natural frequency.

Accelerometers of the force balance type, that have been developed for seismic work can be applied directly to measuring dynamic response of offshore towers to wind and wave forces. These devices are capable of resolving 10^{-6} g's, one millionth of the acceleration of gravity. The Buzzards Bay Tower, in extremely calm weather conditions, responds at 10^{-5} to 10^{-4} g's at its natural frequencies. Much of the instrumentation that works on buildings is readily adaptable to offshore towers.

Fast Fourier Transform techniques have been used to analyze the dynamic response of offshore structures. E.H. VanMarcke (4) has shown that from FFT spectral analysis of acceleration records accurate estimates of natural frequency and modal damping can be obtained for offshore towers. Fast Fourier Transform spectrum analysis was employed in this work to obtain estimates of natural frequency and damping.

III. INSTRUMENTATION

A. Testing Theory

The lowest frequencies of vibration that are found on bottom supported towers in the ocean are the flexural and rotational frequencies associated with the bending and twisting of the entire structure relative to the point of bottom attachment. These frequencies are important for structural reasons, because they are low enough to be driven by the higher frequency components of the wind and wave force spectra. Moreover, because they result in relatively large periodic motions of the entire structure, they represent a significant source of cyclic stress on the major supporting members. Under certain resonant conditions these vibration modes can be responsible for widespread structural failure. Monitoring these modes yields information pertinent to the integrity of the entire structure. Although it is possible to measure the natural frequencies of individual plates, columns and beams, the results are applicable to only those particular members. The emphasis in this work was on the development of an inspection technique that provided a measure of the general integrity of the structure rather than a one at a time inspection of individual members.

The bending or rotational vibration of an offshore tower is usually dominated by a low frequency fundamental with occasional second and even third order frequencies superimposed. The lowest frequency usually dominates because it has more

energy available from the wind and waves than do the higher order modes. In many cases, as with the Buzzards Bay Entrance Tower only the fundamental modes are regularly excited and consequently the measurement and analysis was necessarily confined to the fundamentals. Had the higher modes been excited during any measurement period, they would have been detected and used for comparison to later measurements. The important point is that adequate deductions can be made from the fundamental frequencies only, and the occasional or even continuous superposition of higher modes does not hinder the tests or alter the final results.

B. Instrumentation

Accelerometers: Accelerations caused by the fundamental modes are largest at the top of the tower. The purely translational vibrations can be resolved into two perpendicular components. In the case of a tower with a rectangular planform, and symmetric mass distribution the two flexural motions are parallel to the two principle vertical planes of the structure and the rotational motion is about a vertical axis through the geometric center of the structure. Thoughtful placement of the accelerometers which measure these motions can make analysis of the data relatively simple.

Figure III-1 shows the recommended placement of accelerometers on the top of a tower with a rectangular planform. Looking down on the top of the tower, it is obvious that placement of two

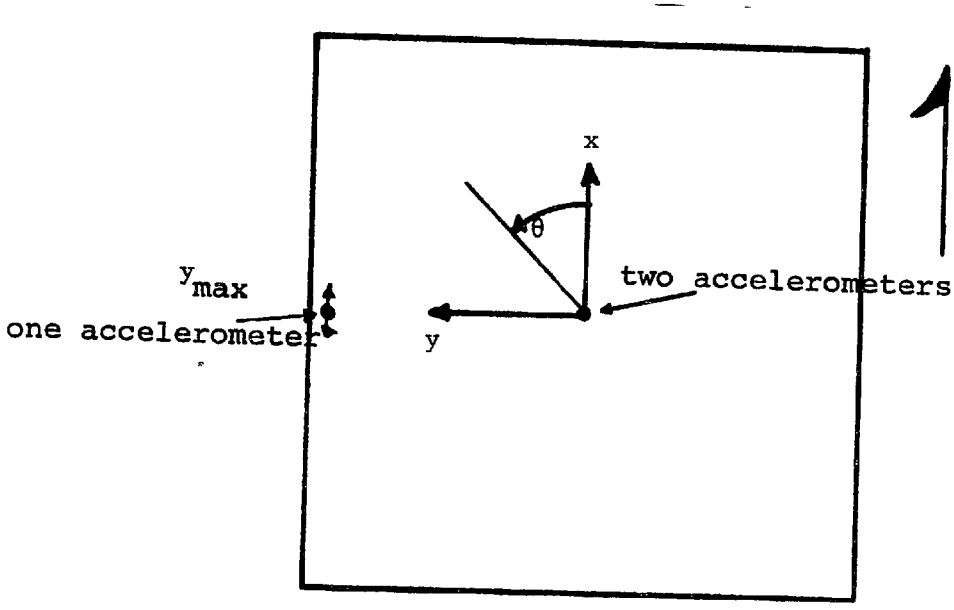

Figure III-1 Accelerometer Placement

accelerometers at the center of rotation, and oriented to measure horizontal accelerations in the x and y directions, allows measurement of the principle $\ddot{x}$ and $\ddot{y}$ flexural accelerations at the top of the tower with no interference from the rotational mode. The placement of a third accelerometer at the extreme y coordinate of the structure, y_{max}, is oriented to measure accelerations that are the sum of the $\ddot{x}$ flexural and the $y_{max}\ddot{\theta}$ rotational components. The Buzzards tower has a square planform with 4 primary steel legs and a symmetric arrangement of horizontal and diagonal braces in the welded steel jacket. The mass distribution in the house at the top of the tower is symmetric in two planes. The symmetry of mass and structure is reflected by two identical x and y flexural fundamental frequencies, and a torsional mode that rotates about the geometric center of the tower.

Recording techniques: The instrument package was designed to simultaneously measure and record accelerations at three locations. The accelerometers used were Endevco QA 116-16 force balance devices that are capable of measuring up to ± 1 g and can resolve down to $\pm 10^{-6}$ g's. They have a sensitivity of 1 volt per g. Numerous other companies make similar devices that are suited to this application. Typical accelerations at the fundamental frequency vary from $\pm 10^{-5}$ to $\pm 10^{-2}$ g's peak to peak depending on weather conditions and structural parameters. A block diagram of the instrument package is shown in Figure III-2. The amplifier gain is 100 and increases the accelerometer output to 100 volts/g. The FM tape recorder is a four channel Tandberg

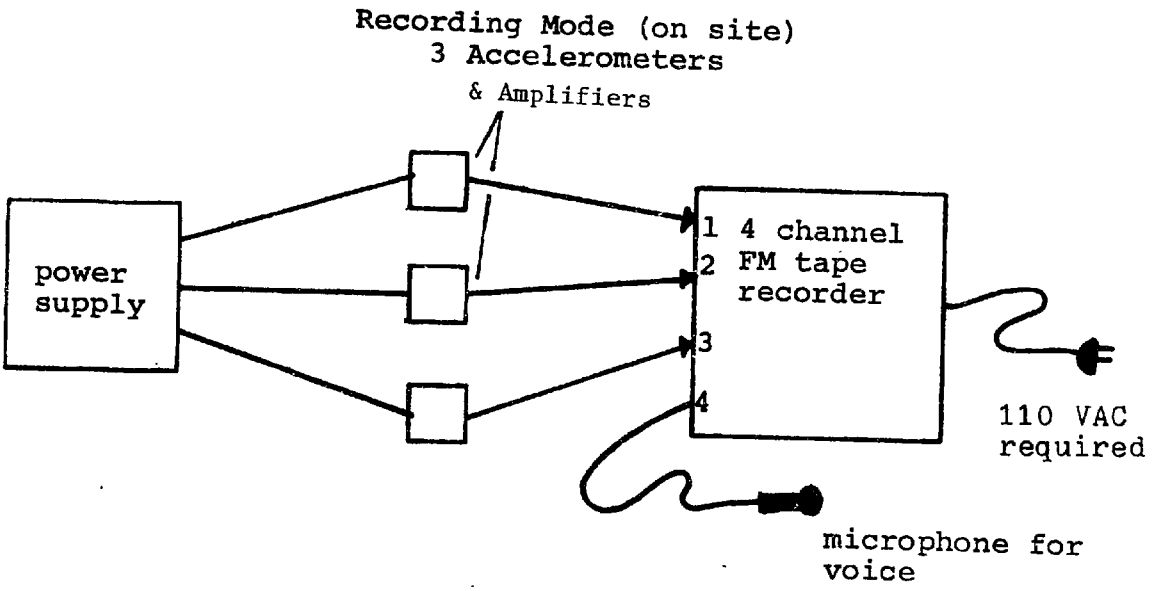

Playback Mode (in laboratory)

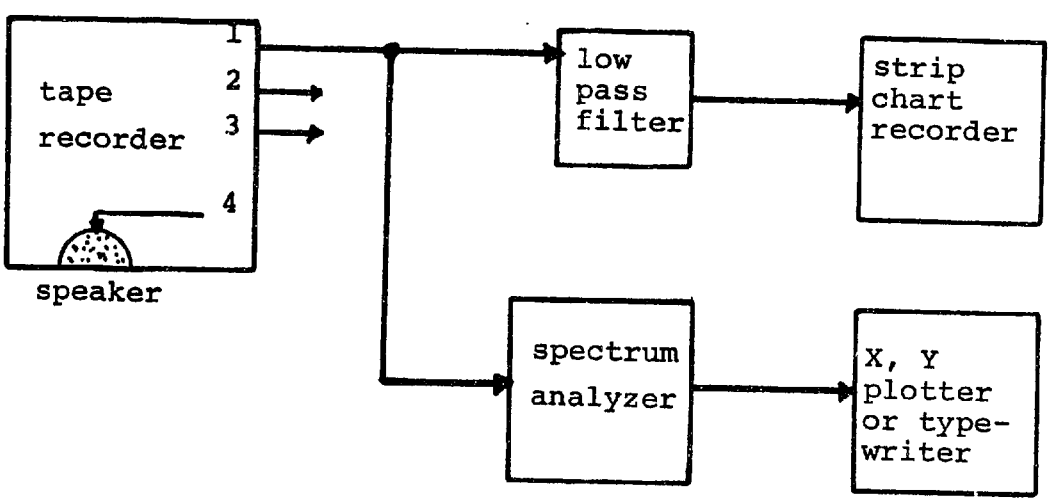

Figure III-2 Instrumentation Block Diagram

Model 100. It uses $\frac{1}{4}$" tape and records simultaneously on four channels. Channel two can be used for flutter compensation and channel four has provision for voice commentary that can be recorded in an over-ride mode. A microphone switch interrupts data collection on the fourth channel allowing voice to be recorded. The total weight of this instrument package is about seventy pounds, including carrying cases, cables and minor accessories. All data was recorded at 1 7/8 inches per second.

Later the data was played back into a spectrum analyzer which identified the natural frequencies. An alternative procedure is indicated by the "optional" dc strip chart recorder that is shown in the block diagram. If the amplified signal from the accelerometer is filtered to remove high frequency noise and then recorded on a sensitive paper recorder, such as a Brush Model 222 , then on the spot determinations of fundamental natural frequency can be made by counting zero crossings over a known length of time. This technique was employed for the 6 May 1974 post collision inspection. Of course the signal from the accelerometer that is placed away from the center of rotation will show a pronounced beating effect that is the result of a linear combination of $\ddot{x}$ and $y_{max}\ddot{\theta}$ accelerations. This problem can be overcome if the $\ddot{x}$ signal from the accelerometer at the center of rotation is electronically subtracted from the accelerometer located at y_{max}.

$$(y_{max}\ddot{\theta} + \ddot{x}) - \ddot{x} = y_{max}\ddot{\theta} \qquad \text{(III - 1)}$$

This can be done using a simple operational amplifier circuit that takes the difference between two incoming signals.

Figure III-3 shows the filtered paper recordings of the $\ddot{x}$ (north-south), $\ddot{y}$(east-west) accelerations from the Buzzards Bay Tower. Figure III-4 shows the signal measured at y_{max} on the west side, $\ddot{x}$, and their difference as explained in Equation III-1.

C. Fast Fourier Transform Techniques

The recordings from the Buzzards Bay Tower were played into a spectrum analyzer located at the Boston Naval Shipyard. The machine was a General Radio/Time Data Model 1923/30 Spectrum Analyzer. It consists of a mini-computer that is hard wired to perform a variety of FFT computations. For the purpose of determining the natural frequencies it was appropriate to have the machine compute power spectra. At the recorded natural frequencies the power spectra reveals sharp peaks. The output from this machine was via CRT display, x y plotter, or teletype. A typical x y recorder output is shown in Figure III-5. The plot is actually composed of discrete points at 0.005 Hz spacing through which a straight line interpolation trace has been automatically drawn. The 0,005 Hz spacing is determined by the input settings on the spectrum analyzer. Of course, finer spacings require longer input records and a larger memory in the computer. The computed spectral values at each 0.005 Hz step are printed out on the teletype on command. From teletype

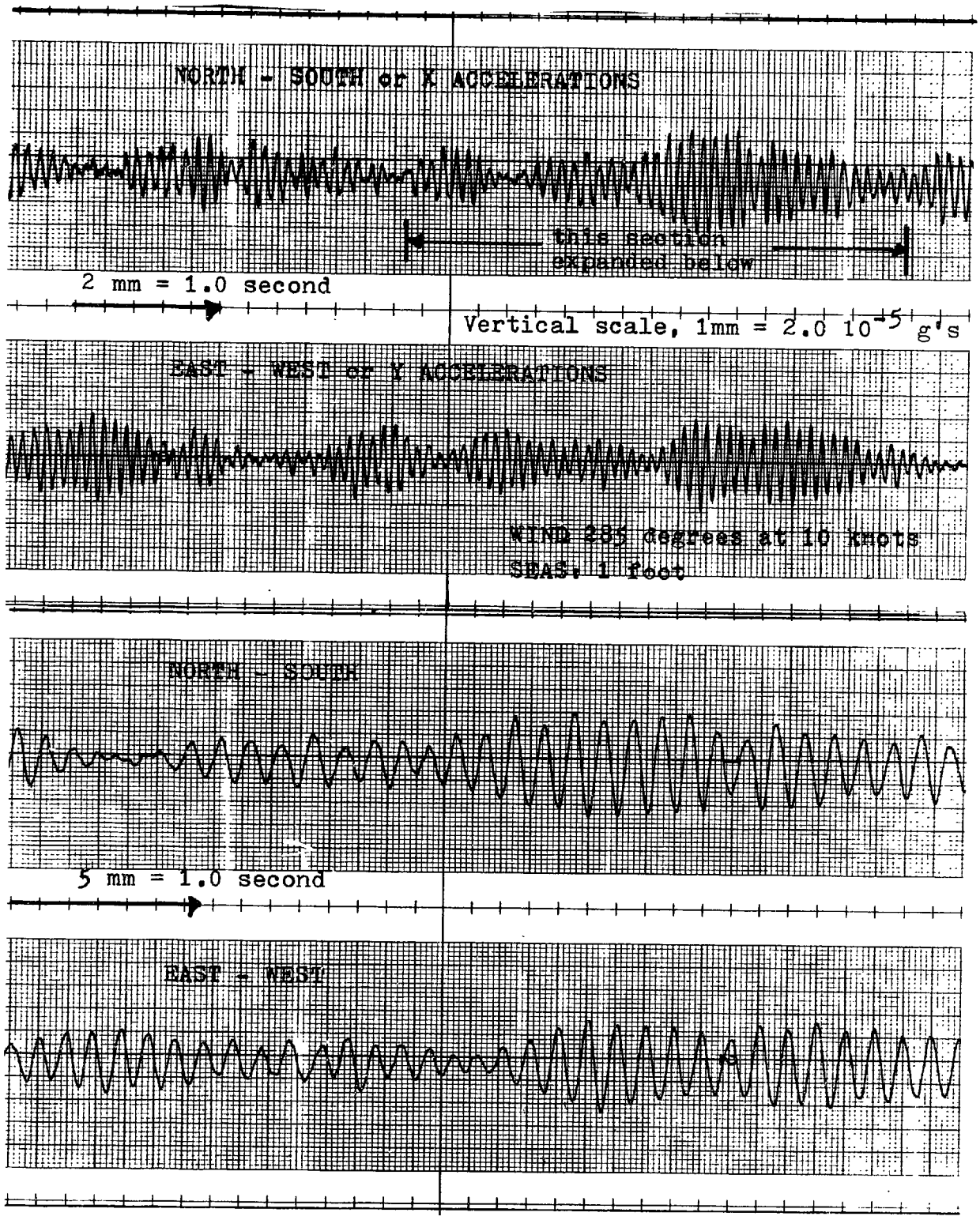

Figure III-3 Sample $\ddot{x}$ (north-south) and $\ddot{y}$ (east-west) Accelerations From the Buzzards Bay Tower

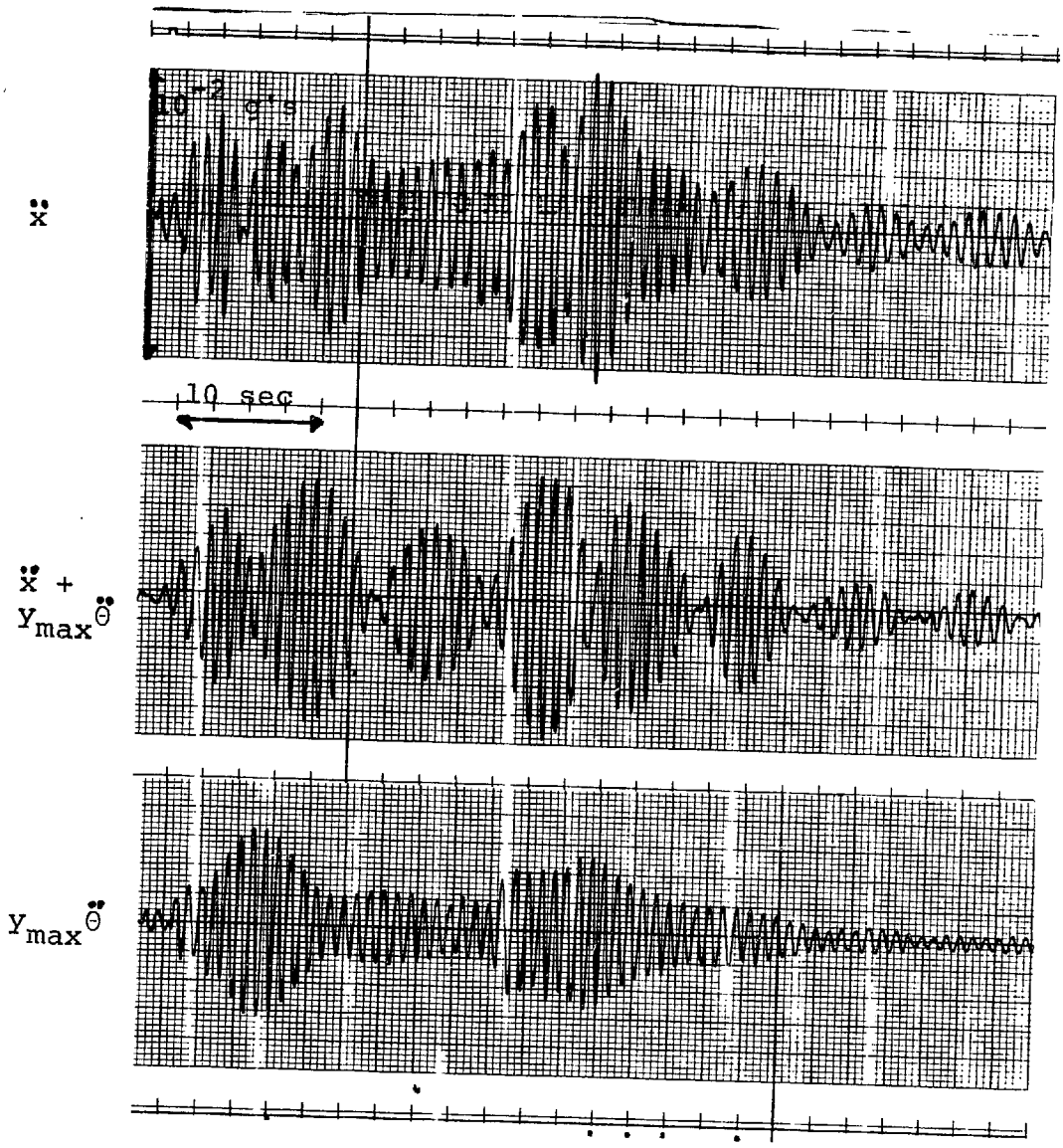

Figure III-4 Sample $y_{max}\ddot{\theta} + \ddot{x}$ Accelerations Separated Into $\ddot{x}$ and $y_{max}\ddot{\theta}$ Components

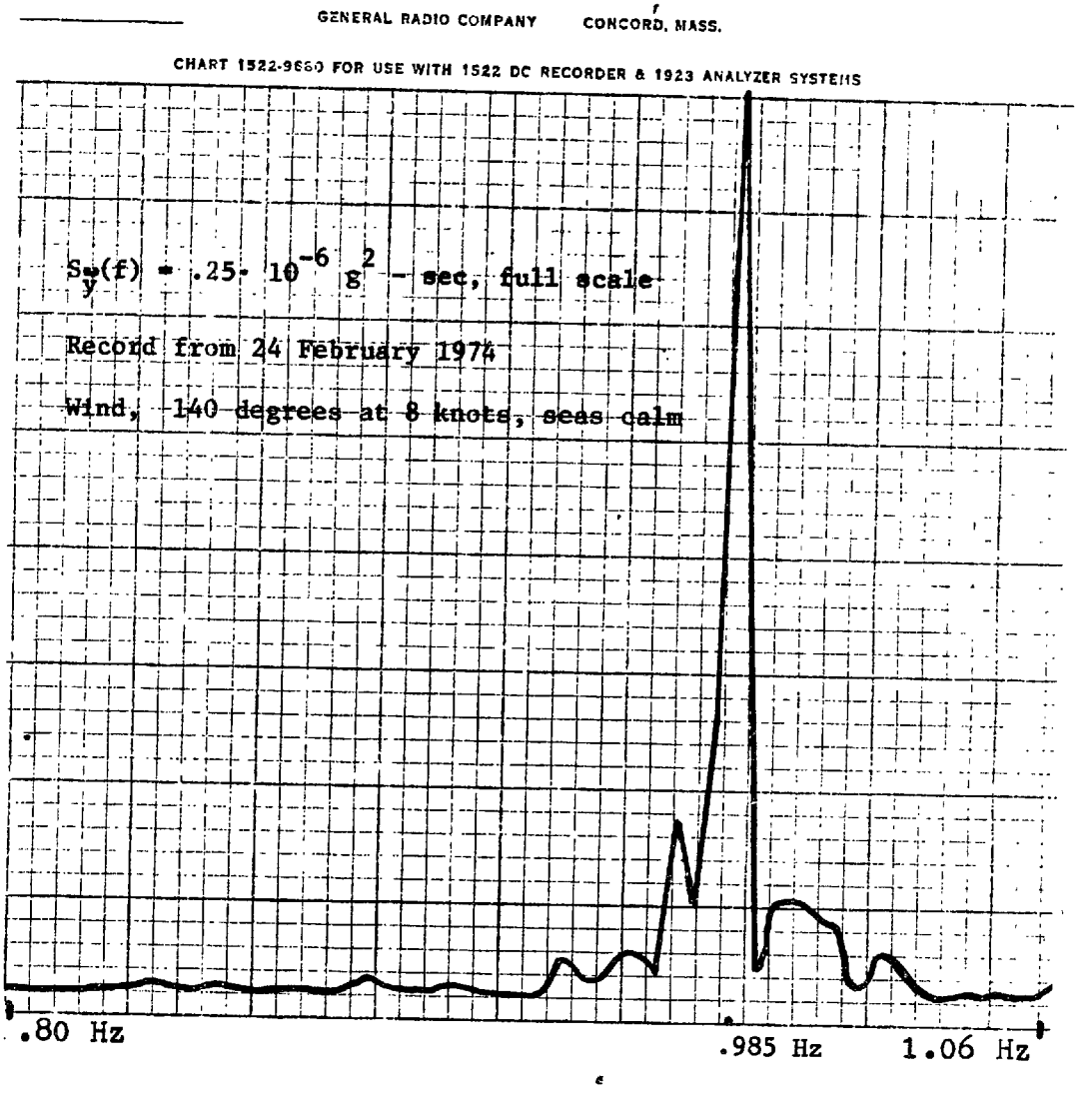

Figure III - 5 Sample Power Spectrum of $\ddot{y}$

output the actual center frequency was determined.

For all tests the spectrum analyzer was set for a full scale range of 0 to 10.24 Hz, with a resolution of 2^9 = 512 data points. The machine automatically observed the Nyquist criterion and actually sampled and computed at 20.48 Hz.

In practice the tape recorder was played back at 7.5 inches per second, which was four times the recorded rate, thus reducing the effective range from 10.24 to 2.56 Hz. This range, when divided by the 512 point resolution, yielded the .005 Hz frequency spacing. Each run required 200 seconds of original data.

From the teletype output the center frequency could be determined as well as the area under the peak which is equal to the mean square value of the signal and hence the acceleration. Though not essential for inspection purposes the mean square acceleration is useful in determining the excitation response relations for the tower. This subject is described in detail in Part II.

In summary the spectrum analyzer was used to determine the natural frequency of a mode to within $\pm$ 0.005 Hz. The recorded data had to be 200 seconds long at 1 7/8 i.p.s. Since the spectrum analyzer treats a signal as a linear combination of sinusoids and resolves the signal into its discrete components at the flexural and rotational frequencies, it automatically resolves the signal recorded at y_{max} into the $\ddot{x}$ and $y_{max}\ddot{\theta}$ components.

D. Detection Threshold

As will be shown, the ability to keep an accurate record of the mass of a particular structure will prove to be the limiting factor in establishing a favorably low detection threshold. However, it is important that instrumentation errors be kept small in relation to mass estimate errors. In a statistical sense the ability to measure the natural frequency depends on the bandwidth of the resonant peak. When measured at the half power points $\Delta f = 2\zeta f_o$. For the Buzzards Tower $\Delta f = 0.02$ Hz. Here ζ is the damping ratio and $\frac{1}{2\zeta} = Q$, the quality factor, which is 50 for the Buzzards Bay Tower. The broader the band width Δf, the more difficult it is to establish an accurate estimate of f_o, the center frequency.

The accuracy of the spectrum analyzer is set by selection of the frequency resolution. For the Buzzards Tower data the power spectra were computed at steps of 0.005 Hz. This spacing is small enough to define the resonant peak with several data points. The accuracy with which the center frequency is determined is ± 0.005 Hz. Averaging the center frequencies, determined from several independent records of course, will improve the estimate of f_o.

The only other important potential source of instrument error is the tape recorder. Tape speed fluctuations cause errors in frequency known as flutter. The Tandberg recorder has $\pm 0.2\%$ tape speed control and even this can be reduced when flutter compensation is used.

When paper recorders are used for on site frequency

measurements, estimates of natural frequency can be made to better than 1% if a machine with a constant paper speed and timing marks is used. Of course longer records yield more accurate estimates.

The total mass of an ocean tower is a critical parameter in establishing its natural frequency. A comparison of the fundamental natural frequency to the simple spring mass system shown below, illustrates the importance of structure mass as well as stiffness.

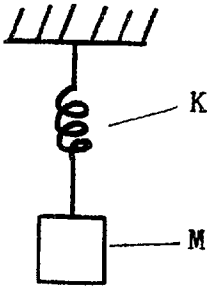

If deflected and released, the mass will oscillate at a frequency given by:

$$f_0 = \frac{1}{2\pi}\sqrt{\frac{K}{M}}$$

Figure III-6 Single d.o.f. Oscillator

Immediately it can be deduced that the frequency varies as $1/\sqrt{M}$. If the mass decreases by 4%, the frequency will increase by 2%. The ability to identify structural damage will be limited by the ability to estimate the change in mass of the structure from the time of the last inspection. On an active drill platform, the amount of mud, drill pipe, water, etc., must all be considered. Marine fouling and underwater flooding of structural members are also potential sources of error which must be detected and eliminated from structural failure considerations.

In order to detect a change in stiffness due to a structural failure we must keep track of the mass. To attribute a change of 2% in natural frequency to a change in structure, we must be able

to keep track of the total mass to better than 4% of the total.

The computer simulation will reveal what the percentage change in natural frequency will be as a function of member damage. The severity of damage that the inspection can potentially detect will be revealed by comparing the computer results to the in-practice ability to detect the long term changes in structure mass. This will vary from one structure to the next. Unmanned producing wells have rather constant mass and hence will have a very sensitive detection threshold. Exploratory drilling sites will have much less sensitive detection limits.

IV. COMPUTER SIMULATION

A. Introduction

Concurrent with the instrumentation program, a computer model was formulated to predict the natural frequencies of the Buzzards Bay Tower. The ultimate purpose of this model was to conduct a parametric study of the effect of simulated structural damage on natural frequency. As it was impossible to actually conduct a systematic survey on a full scale structure, in which members would actually be removed or broken, then it was reasoned that a computer simulation would be the next best thing.

Once the results of the full scale test were in, and the accuracy of the natural frequency determinations was known, then a conparison to the computer simulation would specify the minimum detectable level of damage that this inspection technique would be able to resolve.

Like a cantilever beam, a pile supported tower has a theoretically infinite number of flexural and rotational natural frequencies. For a spatially complex structure like an offshore tower, with large variations in mass distribution, a standard way of estimating natural frequency is by developing a lumped mass model with a finite number of masses and an equal number of degrees of freedom.[5,6,7] Such models generally predict the lowest natural frequencies most accurately, and yield progressively less accurate estimates of the higher modes. In modeling the Buzzards Bay Tower it was important that the computer simulation be able to predict with reasonable accuracy all of the observable natural frequencies. It was also desirable

to use a computer model that had the fewest number of degrees of freedom, i.e. lumped masses, so as to keep computer costs to a minimum. It was known from measurements made in 1963 that the fundamental natural frequencies of the tower in flexure and rotation were approximately 1 Hz and 1.1 Hz, respectively, and that higher modes had not been detected. (8)

B. Three Degree of Freedom Lumped Mass Model

Initially, the tower was modeled for flexural modes as a lumped mass system having three masses and, hence, three degrees of freedom and three natural frequencies. Figure IV-1 depicts the tower as it is modeled by this approach.

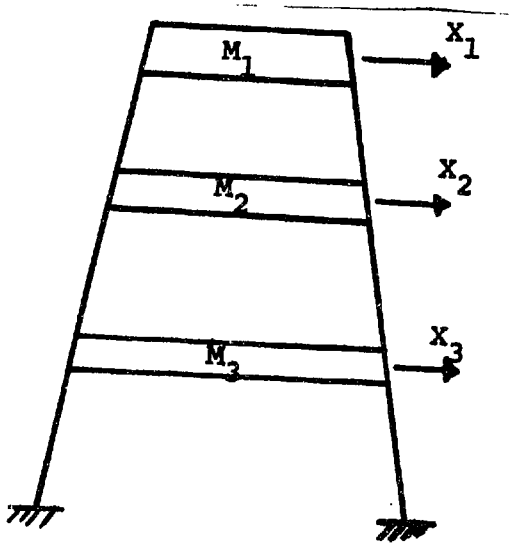

M_1 is the mass of the house and equipment at the top of the tower. M_2 and M_3 have the lumped mass equivalents of the supporting structure. These masses were estimated from blueprints.

FIGURE IV-1 Three d.o.f. Model

The matrix formulation for this problem is as follows:

$$[K]\{X\} = \omega^2 [M] \{X\} \qquad \text{(IV-1)}$$

where [K] and [M] are the stiffness and mass matrices respectively, and {X} is the eigenvector $\begin{Bmatrix} X_1 \\ X_2 \\ X_3 \end{Bmatrix}$ which describes the relative displacements of each of the masses for each of the three natural frequencies. The three values for ω^2 which satisfy this equation are the eigenvalues and are also the squared values of the three natural frequencies in radians^2/sec^2. We can express the natural frequencies in cycles per second or Hertz by $f = \omega/2\pi$.

The stiffness matrix [K] was determined using the ICES-STRUDL II[2] structures program. The pertinent structural details were taken from the construction blueprints of the Buzzards Bay Tower. The nine element stiffness matrix was generated using the principle of superposition. In short, two out of the three masses are held fixed while the third is given a unit displacement. The force required to displace one mass is one stiffness element, and the forces required to hold the other masses fixed are two additional stiffness elements. The other six elements are generated by displacing each mass in turn while holding the remaining two fixed. This method is described very well in a paper by Mansour and Millman[5]. The STRUDL program is discussed in greater detail in section III.D..

The mass matrix [M] is a three element diagonal matrix consisting of the three lumped masses which were estimated from construction specifications.

A standard IBM Scientific Subroutine program was used to solve the matrix equation for the eigenvalues and eigenvectors. The natural frequencies and mode shapes predicted by the program were:

$f_1 = 1.00$ Hz	$f_2 = 8.7$ Hz	$f_3 = 23.0$ Hz
$x_1 = 1.0$	$x_1 = -0.03$	$x_1 = 0.02$
$x_2 = 0.29$	$x_2 = 1.0$	$x_2 = -0.86$
$x_3 = 0.05$	$x_3 = 0.95$	$x_3 = 1.0$

Since the tower has a square symmetric planform, these natural frequencies will be identieal for both X and Y flexural vibrations. The three rotational natural frequencies can be similarly predicted.

The eigenvectors $\{x\}$ represent the mode shape, or relative maximum displacements for each of the three natural frequencies. The deflections are normalized so that the largest is 1.0. The movement of the other two masses is some fraction of the largest deflection. A minus sign indicates movement in the opposite direction; i.e., 180° out of phase. So, for example, the mode shape for the fundamental natural frequency f_1, is a simple bending of the structure. The top mass moves the farthest with the two lower masses leaning in the same direction but to a lesser degree. The bottom of the structure is, of course, fixed and does not move. It is known that the flexural natural frequencies for this type of structure are approximately related as follows:

$$\frac{f_n}{f_1} = (2n-1)^2 = 1, (3)^2, (5)^2 \ldots \qquad \text{(IV-2)}$$

The computed values for the first three flexural modes are

$$\frac{f_n}{f_1} = 1, 8.7, 23$$

which is in close agreement, thus giving added confidence to

the model.

Acceleration data was collected for both flexural and rotational motion on the Buzzards Bay Tower in weather conditions varying from calm to 55 knot winds and 16 ft. seas. The FFT spectral analysis indicated that the fundamental natural frequencies for the two flexural and one rotational mode were the only ones excited; the higher modes were not. There is good physical reason for this. First, the energy content of the wind and wave forces at 1 Hz is small, and drops off very rapidly with increase in frequency. Secondly, 90% of the total mass of the tower is concentrated at the top. One might expect that the motion would be dominated by the fundamental oscillation of this single lumped mass.

This evidence gave credence to the belief that a single lumped mass single d. o. f. model would adequately describe the motion of the BBT.

A single d. o. f. model was specified to STRUDL and the result as predicted by:

$$f_o = \frac{1}{2\pi}\sqrt{\frac{K}{M}} = 0.98 \text{ Hz}, \qquad \text{(IV-3)}$$

which differs from the three d. o. f. model by only 2%. To come within a few per cent of the actual measured natural frequency gave added confidence in the STRUDL structures program, and in the single d. o. f. model. The single d. o. f. model is described in detail in the next section. It was used to calculate the change in natural frequency due to member failure.

C. Single Degree of Freedom Model

The single degree of freedom model is shown in idealized form in Figure IV-2.

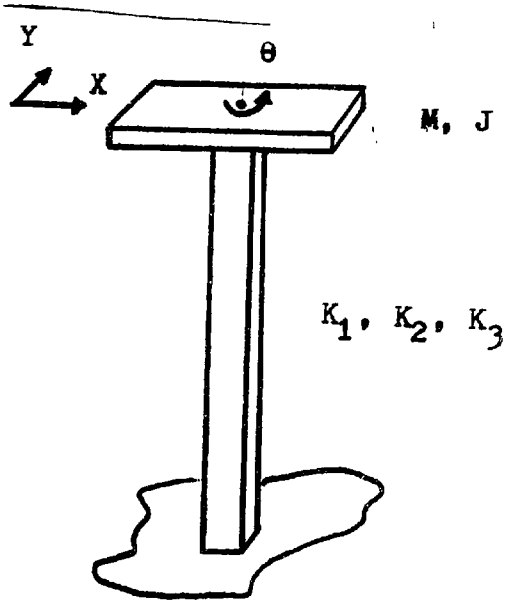

Figure IV-2 Single d.o.f. Tower Model

If displaced and released in the x or y directions, the mass will oscillate at a frequency given by:

$$\omega_x = \omega_y = \sqrt{\frac{K_1}{M}}$$

where: M = mass

$K_1 = K_2$ = flexural spring constant

If rotated and released, the mass will oscillate in torsion at its rotational natural frequency as given by:

$$\omega_\theta = \sqrt{\frac{K_3}{J}}$$

where: K_3 = torsional spring constant

J = moment of inertia

Both M and J can be evaluated directly from the construction specifications of the tower. The STRUDL program is used to evaluate K_1, K_2 and K_3. In preparing the final form of the STRUDL program ω_x, ω_y and ω_θ were known. The principal problem was to specify a computer model that would yield the proper K_1, K_2 and K_3 so that the measured and computed natural frequencies would agree. In practice it is relatively easy to specify a model that yields a good prediction for the flexural or rotational spring constants, but not both. The reason for this is that a pile supported structure is not accurately modeled by assuming that the tower is built in or fixed to the bottom. In fact the soil exhibits an elasticity that varies with depth and load.

STRUDL can compute the stiffness of a space frame quite well for the built-in condition, but does not have any provision to account for the influence of soils. The programmer is left to approximate the soils by groups of springs attached to the bottom sections of the tower. This was done for the STRUDL model of the tower, and Figure IV-3 shows the model with springs in place. The spring constants were selected after reading the most recent publications on laterally loaded piles in sand[9], and by the rather pragmatic approach of using the spring coefficients that yielded the best result. The model as shown was chosen as it gave acceptable predictions and yet did not require a large number of joints at which springs were attached. Increasing the number of springs would have increased the accuracy at the expense of considerably more computer time.

As stated before the natural frequencies in flexure and rotation were 1 Hz and 1.1 Hz. The computer model predicted 1 Hz and 1.4 Hz. The frequency in torsion is 30% high. By current standards for models of this type, the agreement is really quite good. Since the per cent change is frequency due to structural damage is the parameter of real interest in this study, and not the absolute value of the frequency then the absolute error is not critically important.

D. STRUDL Model

The input to the STRUDL II space frame analysis program is shown in Appendix I. They include joint locations, member identification and properties, support conditions, and loadings. The output for this application was limited to printing the applied loads, which in this program were actually unit displacements, and listing the reaction at the joints to the applied displacements. Figure IV-3 shows the STRUDL model of the tower. The three digit numbers identify members.

Determination of the spring constants K_1, K_2 and K_3: When unit displacement is specified in the +X direction at the top of the tower, the STRUDL program computes the reaction force at the joints where the displacement was specified. This force is the spring constant K_1 with units of force/unit deflection. Similarly, a unit displacement in the y direction will yield K_2. For an undamaged tower, $K_1 = K_2$. If an angular deflection is imposed at the top of the tower, then from the reactions the

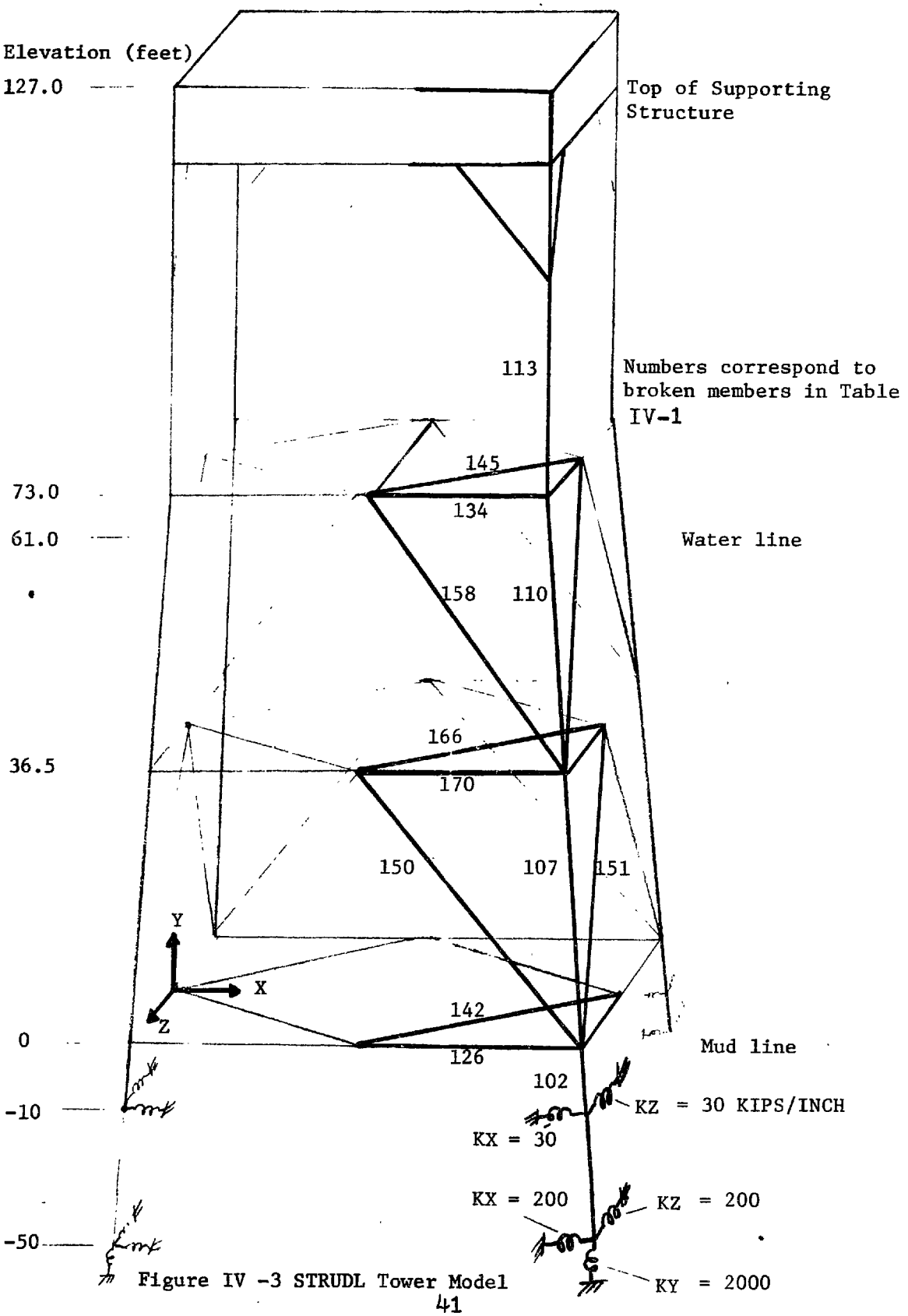

Figure IV -3 STRUDL Tower Model

moment can be calculated, and therefore K_3 in units of ft-lbs/radian. These values can be used directly in equations IV-4 and IV-5 to compute the natural frequencies ω_x, ω_y and ω_θ.

Damage Simulation: STRUDL allows the user to declare members inactive prior to applying the load. If, for example, member 150, a "K-brace', was declared inactive, the stiffness would be computed as if member 150 were removed, or completely severed. Of course, since member 150 provides more rigidity in the x direction than it does in the y, then K_1 will be smaller than K_2, and ω_x will be less than ω_y. Consequently, on a real tower, a detected change in natural frequency in the x mode, but not the y, would isolate a suspected break to those members contributing to the stiffness in the x direction.

In turn, each of the important members in one quarter of the tower was declared inactive, and the resulting changes in K_1, K_2 and K_3 were computed. These results are tabulated in Table IV-1 in terms of the per cent reduction in natural frequency caused by the simulated damage. Because of symmetry, it was not necessary to simulate breaks in the other three quarters of the tower.

Steel wastage: Since the properties of each individual member must be specified, it is possible to simulate the effect of rust on stiffness. For one stiffness calculation, 0.050" of rust was specified over the entire submerged portion of the structure. The upper portion of the Buzzards Bay Tower is painted. The resulting significant change in natural frequency is tabulated with the rest. 0.050" does not sound very large until compared to the wall thickness of many members. One inch is the largest

wall thickness, and many are as low as 0.322". The resulting reduction in cross-sectional area and moments of inertia of the steel cylinders is significant.

Damaged Member (See Figure IV-3)	Per Cent Reduction in Frequency			Is Damage Detectable? (See Section V)
	f_x	f_y	f_0	
None	0.0	0.0	0.0	N/A
102	17.14	17.14	12.13	Yes
107	11.15	11.15	0.17	Yes
110	5.92	5.92	0.96	Yes
113	8.80	8.80	6.62	Yes
126	0.12	0.0	0.03	No
142	0.005	0.005	0.02	No
150	6.10	0.17	2.25	Yes
151	0.17	6.10	2.25	Yes
166	0.005	0.005	0.008	No
170	3.19	0.0	1.36	Yes
158	7.18	0.0	2.05	Yes
134	3.31	0.0	2.08	Yes
145	0.008	0.008	0.005	No
0.050" Rust	3.71	3.71	1.41	Yes

For no damage: $K_1 = K_2 = 59.554$ KIPS/INCH

$K_3 = 1.58 \times 10^6$ FT-KIPS/RADIAN

TABLE IV-1. Reduction in Frequency Due to Member Removal and Steel Wastage

Detectable changes: The problem now reduces to one of determining the accuracy to which measured changes in natural frequency can be attributed to changes in stiffness. As pointed out in Section III-D, if the mass of the tower can be

estimated to only $\pm 4\%$ from visit to visit, then changes in stiffness of less than $\pm 4\%$ may be impossible to isolate. In the next section the BBT's mass estimates are shown, and the damage detection threshold is determined.

V. MASS, MOMENT OF INERTIA, AND THE DETECTION THRESHOLD

A. Instrumentation Limitations

As discussed in the section on Instrumentation (III-C), a computation resolution of 0.005 Hz was selected for the spectrum analyzer. This was a compromise which gave several data points over the bandwidth of the resonant peak ($\Delta f_{\frac{1}{2}\ \text{power}} = 0.02$ Hz) and yet did not require awkwardly long recordings of tower acceleration (T = 200 seconds) or exceed the memory capacity of the spectrum analyzer.

For the Buzzards Bay Tower a reasonable goal for the detection threshold would be the ability to attribute changes in natural frequency of greater than $\pm$0.005 Hz to changes in mass or stiffness. Since frequency varies inversely with the square root of the mass, it is necessary to keep track of the mass to better than $\pm$1% to achieve this goal.

B. Mass and Moment of Inertia Estimates on the Buzzards Bay Tower

One percent of the total mass and moment of inertia of the BBT are respectively 200 slugs and $2 \cdot 10^5$ slug-ft^2. These quantities must be compared to the errors involved in estimating the change in M and J from one visit to the next. The sources of change between visits are listed below:

1. Added mass due to changes in tidal level, and flooding of submerged members.
2. Changes in stores, equipment and personnel.
3. Accumulation of marine growth.

4. Presence of a helicopter.

5. Accumulation of rain, snow or ice.

6. Change in quantity of fuel oil and fresh water on board.

Compared to $\pm$1% of M and J, the error in estimating items 1, 2 and 3 are small. Item 4, a helicopter, could be accounted for, but the data presented here was collected after departure of the helicopter. Due to the difficulty of estimation, measurements must not be taken at times of heavy snow and ice accumulation.

Item 6, fuel and fresh water are the only serious sources of error on the BBT. As much as 40% of the total mass of the tower can be liquid. Although the exact amount can be easily determined, these liquids can not be treated as rigid body masses. They are stored in four identical rectangular tanks, arranged as shown in Figure V-1, and located directly beneath the living quarters. Even when full the tanks have a free surface. The natural frequencies of the first three standing wave modes in both x and y directions are usually lower than 1 Hz. The frequencies are of course depth dependent, but in general the mass of the liquid is vibration isolated from the motion of the tower, and usually the effective mass, i.e., the rigid body equivalent, is approximately 1% of the total. Calculations and experiments performed by Vandiver[10] in 1968 show that the effective mass of an oscillating rectangular tank of liquid is given by:

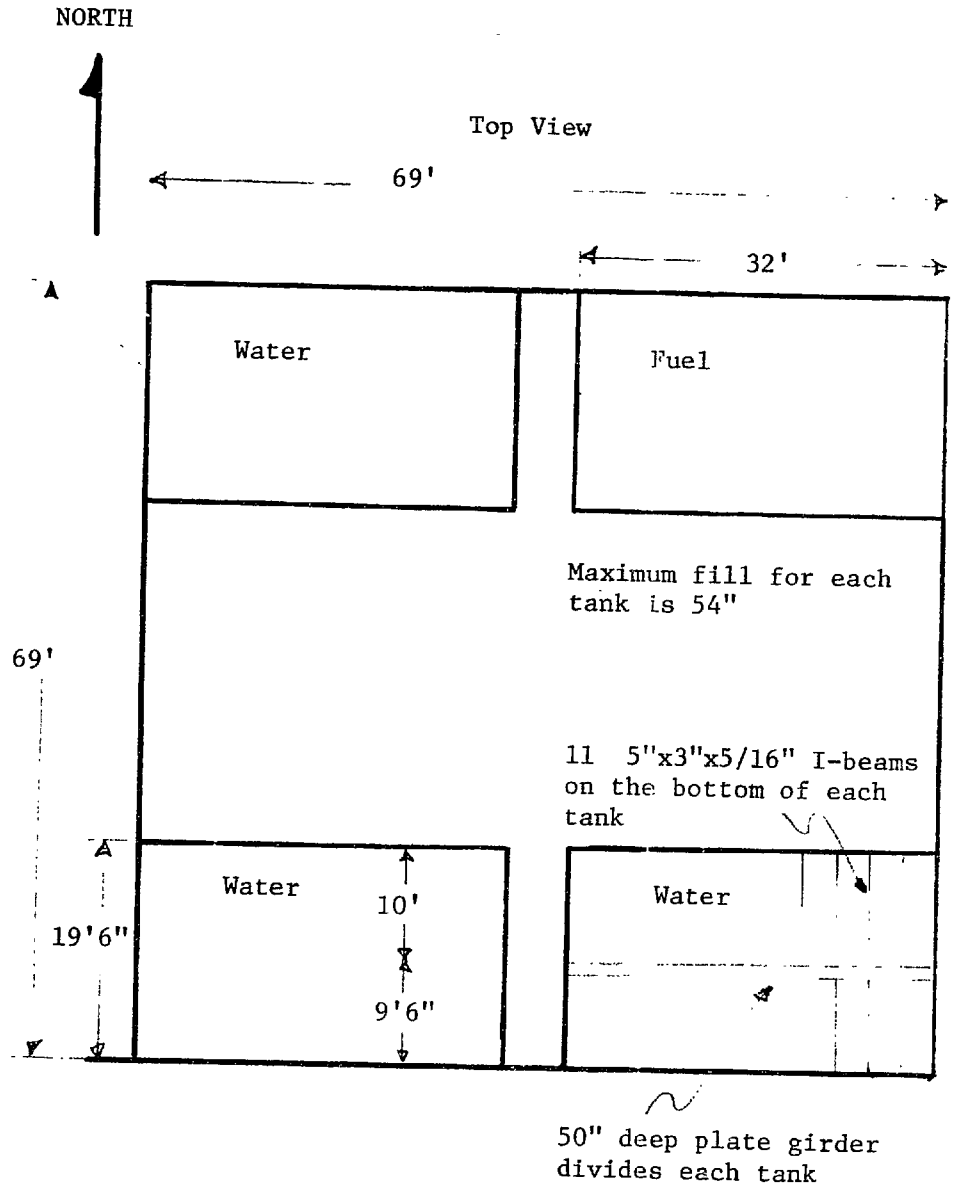

Figure V - I Fuel and Water Tanks on the BBT

$$M_e = M_{total} \sin \omega t \left\{ 1 + \sum_{\substack{n=1 \\ \text{for } n_{odd}}} \frac{\frac{8}{n^2\pi^2} \frac{L}{n\pi h} \tanh \frac{n\pi h}{L}}{\left[\frac{\omega_n^2}{\omega^2} - 1 \right]} \right\} \qquad \text{(V-1)}$$

where: $\omega_n^2 = \frac{n\pi g}{L} \tanh \left(\frac{n\pi h}{L} \right)$

n = 1, 3, 5 ...
h = tank depth
L = driving frequency
ω_n = natural frequency of standing wave
g = acceleration of gravity

Calculations using this equation support the observation that only about 1% of the mass of the liquid need be included in the natural frequency computation. It was not possible to rely completely on the prediction of Equation V-1, because the tanks on the tower were not ideal rectangular boxes. Each tank was divided by a baffle which did not extend all the way to the bottom, but rested on I beams which crossed the floor of the tank at regular intervals. Of course the equation does not account for viscous effects either.

The observed effective moment of inertia of the liquid was about 23% of the total. Table V-1 shows the predicted values for the three fundamental frequencies, based upon 1% and 23% of the liquid mass and moment of inertia. These values are compared to the measured values on each of four visits to the tower. The standard deviation for natural frequency measurements was about 0.005 Hz. (based on 50 separate measurements each of f_x, f_y and

f_θ). As demonstrated by this table, the goal of accounting for changes in frequency to $\pm$0.005 Hz was achieved for f_x, but f_y and f_θ were predicted to an accuracy of $\pm$ .01 Hz. It is evident that large amounts of liquid storage is a source of serious error. No predicted values are shown for the first visit in Table V-I, because the measured values on the first visit were required to predict changes in frequency based on liquid levels for later visits.

Table V-1 Predicted Versus Measured Natural Frequency For Various Liquid Levels

DATE	PREDICTED FREQUENCY			MEASURED FREQUENCY		
	(f_x)	(f_y)	(f_θ)	(f_x)	(f_y)	(f_θ)
25 Feb 1974	- - - - - - - - - -			.9765	.9831	1.1008
6 May	.9753	.9819	1.0720	.9758	.9784	1.0791
17 July	.9760	.9869	1.0868	.9752	.9874	1.0762
16 Aug	.9759	.9825	1.0855	.9719	.9744	

The mass of the tower other than liquid was obtained by adding the mass of the house, tanks and helicopter deck (total 251 tons) to one half the mass of the supporting framework (40 tons), a total of 291 tons or 18.09×10^3 slugs, and a moment of inertia of 17.36×10^6 slug-ft^2. The effect of the added mass and moment of inertia of the sea water around the supporting structure increases these totals to 18.59×10^3 slugs and 17.86×10^6 slug-feet^2.

For the February 25, 1974 visit the total mass and moment of inertia, including the effective mass of stored liquids, was 18.67×10^3 slugs and 19.78×10^6 slug-feet^2. The values for flexural and torsional stiffness computed by STRUDL were given in Table IV-1. The natural frequencies predicted using these stiffnesses and the above mass and moment of inertia are:

$$f_x = f_y = .985 \text{ Hz}$$

$$f_\theta = 1.375 \text{ Hz}$$

It is apparent from the above table that the measured values for f_y are slightly higher than f_x. This is probably due to structural differences at the top of the space frame. The tower top is constructed more rigidly in the y direction than the x. Due to the large number of members involved, these minor differences were not modeled by the computer program in an effort to improve computational efficiency, at the expense of not predicting this minor difference in frequency.

C. Detection Threshold for the Buzzards Bay Tower

By comparing the above results to Table IV -1, we can see the severity of structural damage that could be detected with confidence above the error level associated with changes in mass. These results indicate that at least for the Buzzards Bay Tower, this is a valid method for detection of member breakage for much of the submerged structure. For large drilling rigs, the ability to account for drill pipe, mud and heavy equipment may be considerably more difficult. For unmanned production platforms, the mass may change very little with time, and a very sensitive threshold might be attained. It is significant for the BBT that the only undetectable breaks occur in small non-load bearing members.

D. Locating Structural Damage

Certainly from the magnitude of the frequency change, a surveyor could obtain an indication of the severity of the damage. In addition, by comparison of the frequency changes between modes one could determine whether or not the damage was in a location that causes stiffness in a predominantly x or y direction. In addition, it is obvious from Table IV -1 that certain types of failure cause the rotational frequency to change more or less than the flexural ones. Of course, the availability of a computer model is important in making such evaluations, but in the absence of a computer model, sound engineering reasoning in comparing frequency changes could reach many of the same conclusions.

VI. SUMMARY

A. Evaluation and Recommendations for Pile Supported Towers

The most important conclusion of Part One is that damage can be detected by measuring change in natural frequency on pile supported towers. The major limiting parameter is not the instrumentation accuracy, but the ability to attribute changes in frequency to changes in mass and not erroneously to changes in stiffness.

On the Buzzards Bay Tower large liquid storage tanks were the limiting factor in establishing the detection threshold. The detection sensitivity could have been improved if the relation between natural frequency and liquid level had been determined empirically. That is, an experiment might have been conducted in which the natural frequencies were measured as the tanks were varied from full to empty. This was not possible on the Buzzards Bay Tower. However, it is the type of experiment that could be included as part of the construction program for other towers, expecially since pile supported towers are likely to be erected with empty tanks, and then filled.

Even without the benefit of complete empirical determination of the effect of liquid storage on the Buzzards Tower, it is evident from the computer simulation that breaks in all but a few of the non-load bearing horizontal members were detectable. Ideally all members would be detectable, but from a structural point of view, if breaks in certain members cannot be detected,

then one hopes that such members will not be likely to fail. Most tower failures are attributed to overload in large storms. The overloads are caused by wave and wind loads at the top of the structure. The passage of a large low frequency wave causes the tower to bend, in a deflection shape that is very similar to the mode shape in flexure for the fundamental mode. The computer model of the BBT was a single d.o.f. model, which considered only the first mode. The spring constant was determined by deflecting the tower near the top and computing the reactions. Since the stiffness changes very little when the non-detectable members are removed, then it can be argued that these members do not carry much load and are not likely to be the ones that fail under large wind and wave loads. So even though these breaks are difficult to detect, they are not likely to be overloaded in extreme weather conditions, or to be responsible for a subsequent catastrophic collapse.

Many pile supported towers are initially used as drilling platforms. Eventually, the drilling is completed and the tower is used for production purposes. During the drilling period, mud, cement, drill pipe, and heavy moveable equipment as well as stored liquids are large variable quantities that are potential sources of error, and may severely limit the usefulness of this technique. However, an important consideration is that during the drilling period, the tower is new, well staffed and probably frequently inspected by divers. The time when this technique may be a real asset is after production has begun, the staff

reduced, the divers moved elsewhere, and the effects of age have become significant. This relatively inexpensive and mobile test could be successfully employed in a periodic inspection program aided by the relatively minor long term changes in mass. When damage is detected, then the divers can be moved in to complete the job. The frequency measurements might yield additional information about the nature or location of the damage.

Due to the mobility of the test equipment, unscheduled inspections could be easily made on towers after severe storms or even collisions with large vessels. One improvement in instrumentation that might aid the surveyor in such circumstances where immediate results are desirable is a portable spectrum analyzer. This would allow real time, on site, accurate determinations of natural frequency.

B. Extension of Results to Other Offshore Structures

The large reinforced concrete towers under construction for use in the North Sea are one of the most promising candidates for this testing technique. It is likely that micro-cracks in the concrete may cause large frequency shifts, much like those observed in earthquake damaged buildings[3]. Micro-cracks defy visual inspection, especially underwater. Difficult weather conditions and deep water amplify the difficulties associated with diver conducted inspections. For this type of tower, under these circumstances, this technique may be particularly useful.

Jack-up rigs and semi-submersibles are in wide use today. Jack-ups may be difficult to test, because they frequently change configuration, and even position to compensate for uneven settling into the soils. The related changes in center of gravity, soils interaction and stiffness may well cause unacceptable errors.

The semi-submersible introduces an entirely new, though not necessarily insurmountable, set of problems. Since they are floating and not fixed, the natural frequencies of interest are the flexure and torsion of the vessel independent of the bottom. Measurement of these frequencies is complicated by the presence of rigid body oscillations in heave, pitch and roll. An advantage of the semi-submersible is that its mass can be estimated directly from its displacement on any visit. Diver inspections are more easily conducted on semis because they extend to relatively shallow depths. The added capability of periodic dry docking makes them an even less attractive candidate for this inspection technique.

Of the 2,000 plus offshore structures in use today, many are suited to this inspection technique. Its mobility and low cost make frequent inspections possible, even on relatively low priority shallow water producing platforms.

PART II

EXCITATION-RESPONSE ANALYSIS OF THE BUZZARDS BAY TOWER

VII. INTRODUCTION

The sources of environmental loads on offshore structures include wind, waves, current, ice and seismic activity. Under certain conditions each of these can be the source of structural failure and must be considered in the design of offshore towers. The current boom in offshore construction has generated a need for better methods of estimating these loads, and in some cases for estimating the response of the structures to loads. For some types of loads it is sufficient to consider quasi-static response, while for others it is necessary to estimate the dynamic response.

In this investigation the dynamic response to random wind and wave forces was considered. One fixed offshore tower was studied in detail and the measured response data spans a wide range of wind and sea state conditions. The response data is presented and analyzed in the following sections. Also presented are predicted estimates of the response.

The predicted response to random wind loads was estimated using the results of classical random vibration theory. The wind force spectrum was derived from the wind velocity spectrum using methods that have been developed by civil engineers for estimating wind forces on structures.[11,12,13]

The predicted response to random wave loads was calculated from the results of Statistical Energy Analysis. This procedure is a departure from current practice in the offshore industry. Current practice relies almost exclusively on traditional random vibration theory. This requires that a wave force spectrum for each structure be derived from the wave height spectrum and the structural details in the wave force zone. Typically, the force due to a single sinusoidal wave is calculated using the Morrison wave force equation; and the results are generalized to the random wave condition. These calculations necessarily involve the structural details, and hence, complicated structures require tedious calculations and numerous approximations.

Statistical Energy Analysis provides a means for estimating the maximum energy that a resonant structural mode may have, independent of the structural geometry and dependent only on the wave height spectrum and frequency. Furthermore, if the ratio of the modal damping due to generation of waves to the modal damping due to all other sources can be estimated, then the actual mean response energy can be predicted.

Since SEA relies heavily on the general results of random vibration theory, some of the pertinent random vibration concepts are reviewed in Section VIII. As indicated above, damping plays an important role, and the damping estimates from the Buzzards Tower are presented in Section IX. Section X presents the predicted wind response calculations for the Buzzards Tower; and in Section XI the expression for maximum modal energy due to

random wave excitation is derived from SEA considerations, and is independently derived from basic theory regarding resonant structural response to random waves.

In XII the predicted total response to random wind and wave forces is compared to the measured response data for the Buzzards Tower with satisfactory agreement. SEA is shown to be a valid method for predicting the response of offshore structures to random waves.

VIII. RESPONSE OF A SINGLE DEGREE OF FREEDOM RESONATOR TO A RANDOM FORCE

A. Applicability to the Buzzards Bay Tower

The BBT has three dominant modes of vibration, the two flexural modes at 0.975 Hz and a single rotational mode at 1.1 Hz. All three modes are continuously excited by random wind and wave forces. The amplitude of response is related to the amplitude of the excitation, but the modal frequencies of the structure's resonant response are solely dependent on the mechanical properties of the tower. The average response amplitude of each mode is independent of wind and wave direction. The two flexure modes have an equal average modal energy, which is also equal to the average torsional mode energy.

The two flexural modes are weakly coupled to one another by mechanical connections in the structure and because their natural frequencies are essentially identical. The rotational mode shows very little evidence of coupling, because its resonant frequency is significantly different from the flexure frequencies. The properties of small or no coupling and approximately equal average modal energy make it possible to analyze the three resonant modes as if they were each an independent single degree of freedom resonator. In the following discussion a single d.o.f. mathematical model is described. It is used to predict the response of the Buzzards Bay Tower to random wind and wave forces.

B. Random Excitation of a Single Degree of Freedom Mechanical Resonator

Figure VIII-1 depicts a single d.o.f. mechanical resonator. Equation VIII-1 is the well known second order linear differential equation which describes it.

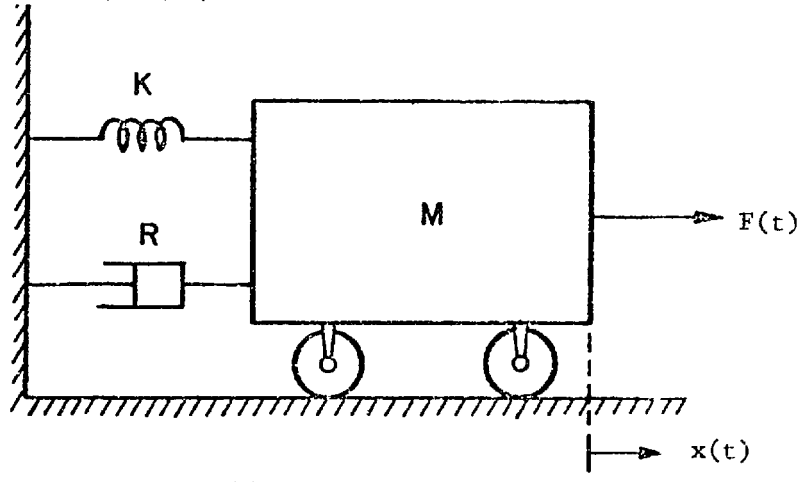

FIGURE VIII-1 Single d.o.f. Resonator

$$M\ddot{X} + R\dot{X} + KX = F(t) \qquad \text{(VIII-1)}$$

where: M = lumped mass equivalent of tower
R = mechanical resistance
K = spring constant K_1 or K_2
F(t) = driving force

This equation will be used to describe the two flexural modes. The appropriate differential equation describing the torsional mode is:

$$J\ddot{\theta} + R_3\dot{\theta} + K_3\theta = T(t) \qquad \text{(VIII-2)}$$

where: J = moment of inertia
R_3 = mechanical resistance
K_3 = torsional spring constant
T(t) = driving torque

The two equations are identical from a mathematical viewpoint, and henceforth only the first will be discussed, but application of conclusions to the torsional case are obvious extensions of the solution. The response of this system to random excitation is well known[14] and the details pertinent to this discussion are summarized below.

The Fourier transform description of the excitation response relation for this system is:

$$X(\omega) = H(\omega)\, F(\omega) \qquad \text{(VIII-3)}$$

where: $X(\omega)$ = Fourier transform of the response $X(t)$
$F(\omega)$ = transform of the excitation $F(t)$
$H(\omega)$ = transform of the response $X(t)$ to unit impulse force $\delta(t) = F(t)$

For this mechanical system:

$$H(\omega) = \frac{\frac{1}{M}}{(\omega_o^2 - \omega^2) + 2i\zeta\omega\,\omega_o} \qquad \text{(VIII-4a)}$$

and:

$$|H(\omega)|^2 = \frac{\frac{1}{M^2}}{(\omega_o^2 - \omega^2)^2 + 4\zeta^2\omega^2\omega_o^2} \qquad \text{(VIII-4b)}$$

where: $\omega_o = \sqrt{K/M}$, the natural frequency in rad/sec
ω = driving frequency
$\zeta = R/2\omega_o M$, the damping ratio
$i = \sqrt{-1}$

If the forcing function $F(t)$ is a stationary random process with a single sided power spectrum $S_F(\omega)$, then the following relations are known:

$$E[F^2] = \int_0^\infty S_F(\omega)\,d\omega = \text{mean square force} \qquad \text{(VIII-5)}$$

$$S_x(\omega) = |H(\omega)|^2 S_F(\omega) = \text{displacement response spectrum} \qquad \text{(VIII-6)}$$

$$E[X^2] = \int_0^\infty S_x(\omega)\,d\omega = \text{mean square displacement} \qquad \text{(VIII-7a)}$$

$$= \int_0^\infty |H(\omega)|^2 S_F(\omega)\,d\omega$$

$$E[\dot{X}^2] = \int_0^\infty \omega^2 S_x(\omega)\,d\omega = \text{mean square velocity} \qquad \text{(VIII-7b)}$$

$$\omega^2 S_x(\omega) = S_{\dot{x}}(\omega)$$

$$E[\ddot{X}^2] = \int_0^\infty \omega^2 S_{\dot{x}}(\omega) = \text{mean square acceleration} \qquad \text{(VIII-7c)}$$

$$\omega^2 S_{\dot{x}}(\omega) = S_{\ddot{x}}(\omega)$$

Figure VIII-2 shows the function $|H(\omega)|^2$. The peak becomes sharper as damping is decreased. For low damping the integrals in Equations VIII- 7a, b and c become dominated by the resonant response in the vicinity of the peak in $|H(\omega)|^2$. For $\delta \leq 0.15$ we can use the approximations:

$$E[\dot{X}^2] = \omega_o^2\, E[X^2] \qquad \text{(VIII-8a)}$$

$$E[\ddot{X}^2] = \omega_o^2\, E[\dot{X}^2] \qquad \text{(VIII-8b)}$$

Furthermore, if $S_F(\omega) = S_o$, a constant over the band of the resonant peak in $|H(\omega)|^2$, then the mean square response can be approximated by [14]:

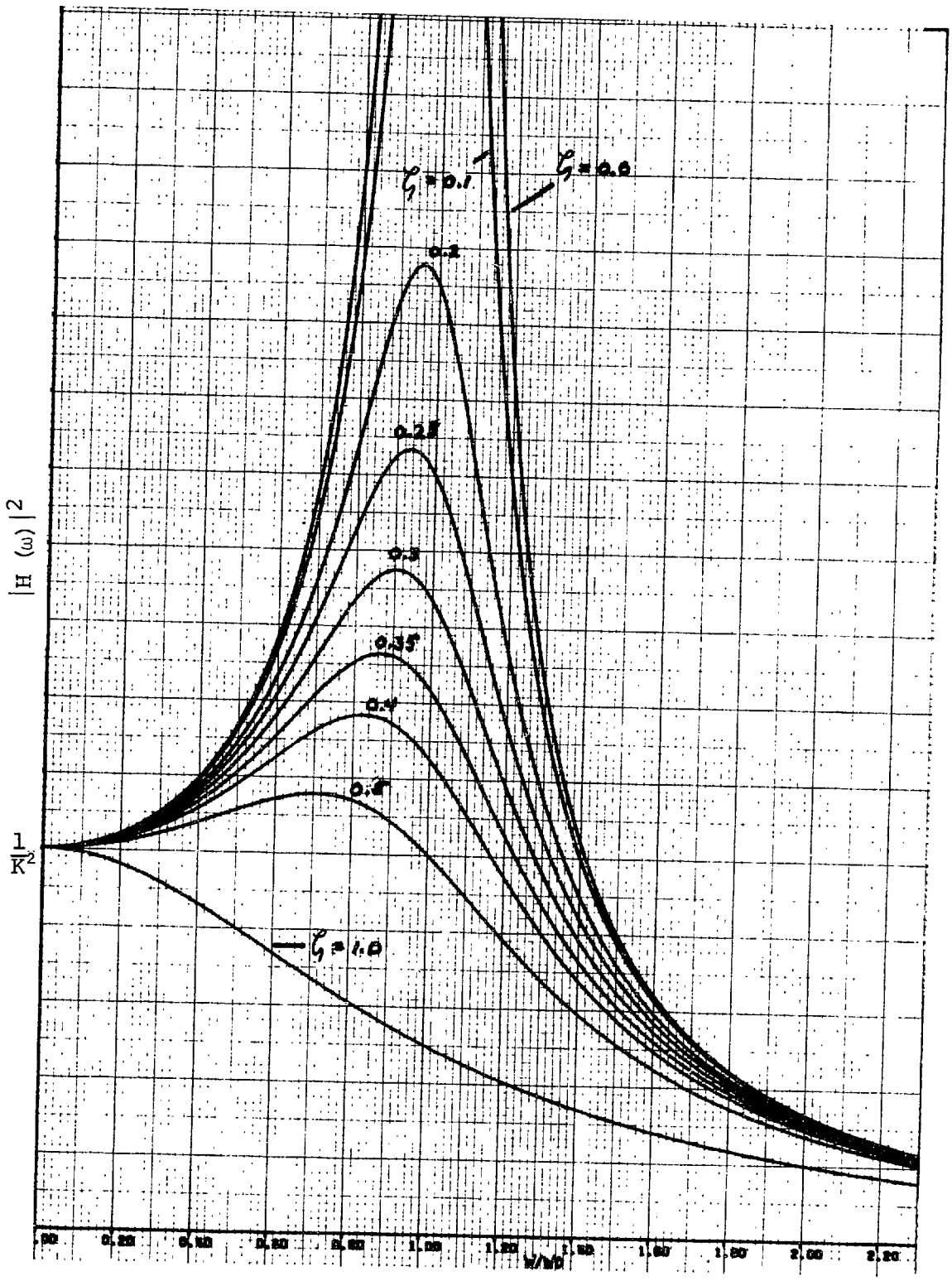

Figure VIII-2 $|H(\omega)|^2$ vs Frequency Ratio ω/ω_o

$$E\,[X^2] = \frac{\pi S_o}{4\zeta \omega_o^3 M^2} \qquad \text{(VIII-9a)}$$

$$E\,[\dot{X}^2] = \frac{\pi S_o}{4\zeta \omega_o M^2} \qquad \text{(VIII-9b)}$$

Since the average energy of the resonator is equal to twice the average kinetic energy, then the expression for average modal energy is:

$$\langle E \rangle = ME\,[\dot{X}^2] = \frac{\pi S_o}{4\zeta \omega_o M} = \frac{\pi S_o}{2R} \qquad \text{(VIII-10)}$$

As will be shown, all three modes of the Buzzards Bay Tower have damping ratios of $\zeta \cong 0.01$, which is so small that the above approximations are very accurate. The halfpower bandwidth of the resonant peaks is 0.02 Hz and over this band the power spectra of the wind and waves can be taken as constant. From Equation VIII-10 the mean modal energy can be calculated for random wind excitation. For random wave excitation some of the random vibration conclusions as well as Statistical Energy Analysis techniques will be employed to predict response.

IX. MODAL DAMPING OF A SINGLE DEGREE OF FREEDOM MECHANICAL RESONATOR

Accurate experimental estimates of damping are in practice difficult to achieve. A common method is to measure the bandwidth of the acceleration response spectrum at the half power points. That is the bandwidth between the two points where the spectrum $S_{\ddot{x}}(\omega) = \frac{1}{2}S_{\ddot{x}}(\omega_0)$ is given by $\Delta\omega = 2\zeta\omega_0$. Unfortunately, the response spectrum is a rapidly changing function of frequency at the half power points, and an accurate estimate of $\Delta\omega$ is not easily obtained. An alternate way is suggested here.

A. Equivalent Bandwidth Approach

The equivalent bandwidth is defined so that it satisfies:

$$S_{\ddot{x}}(\omega_o)\,\Delta\omega_e = E[\ddot{X}^2] \qquad \text{(IX-1)}$$

For the single d.o.f. system discussed here it has been shown[15] that:

$$\Delta\omega_e = \pi\zeta\omega_o \qquad \text{(IX-2)}$$

and therefore:

$$\zeta = \frac{E[\ddot{X}^2]}{S_{\ddot{x}}(\omega_0)\,\pi\omega_0} \qquad \text{(IX-3)}$$

If $E[\ddot{X}^2]$, ω_0 and $S_{\ddot{x}}(\omega_0)$ can all be determined experimentally, then ζ can be calculated. Acceleration records of each mode were analyzed with the spectrum analyzer at the Boston Naval Shipyard. This analysis determined $E[\ddot{X}^2]$, ω_0, and $S_{\ddot{x}}(\omega_0)$ and ζ was calculated. The mean and standard deviation of ζ for

each of the three modes was calculated and is summarized below. The number of measurements from which each of the means was calculated is indicated in parentheses. Values are presented for low excitation conditions (wind $\leq$ 20 knots) and heavier conditions (wind, 30 to 50 knots, seas 6 to 16 feet). There is some indication that the damping increases with amplitude of oscillation, which would be expected for the fluid viscous damping effects of the air and water.

TABLE IX -1 Damping Ratio for the BBT

Mode		X	Y	θ
Low excitation	ζ	.0066(20)	.0061(12)	.0047(17)
	σ_ζ	.0022	.0019	.0014
High excitation	ζ	.0100(12)	.0075(13)	.0065(10)
	σ_ζ	.0047	.0022	.0018

Parentheses indicate the number of values used to compute the mean.

B. Damping Estimate from Records of Transient Decay

If a single d.o.f. system is given an initial displacement, velocity or acceleration, the resulting response amplitude will decay in an exponential fashion, given here for an initial acceleration A.

$$\ddot{X}(t) = Ae^{-\zeta\omega_0 t}\cos(\omega t) \qquad \text{(IX-4)}$$

The peaks of the resulting oscillations fall on the decay envelope $Ae^{-\zeta\omega_0 t}$ at intervals of one oscillation period, $T = 2\pi/\omega_0$. The ratio of two peaks separated by n periods is given by:

$$\frac{\ddot{X}(t)}{\ddot{X}(t + nT)} = e^{+2n\pi\zeta} \qquad \text{(IX-5)}$$

Then for n = 10:

$$\frac{\ddot{X}(t)}{\ddot{X}(t + 10T)} = e^{+20\pi\zeta} \qquad (IX-6)$$

and:

$$\zeta = -\frac{1}{20\pi} \ln\left(\frac{\ddot{X}(t + 10T}{\ddot{X}(t}\right) \qquad (IX-7)$$

The damping on the Buzzards Bay Tower was estimated in this way. During one of the visits to the tower, when the wind and seas were nearly calm, a flexural mode was driven by the author, shifting his weight horizontally in phase with the motion of the tower. In this way the flexural mode was driven to amplitudes in excess of those experienced in 55 knot winds. When the driving force was halted the motion decayed as described above. The top half of Figure IX-1 shows a strip chart recording of $\ddot{x}$ accelerations. On this figure two peaks, ten periods apart, were selected and from Equation 7, $\zeta = 0.0113$ was computed, which is in good agreement with the high excitation value shown in Table IX-1.

C. Modal Coupling

The $\ddot{X}(t)$ record shown in Figure IX-1, was generated by standing at the geometric center of the top of the Buzzards Bay Tower and shifting weight horizontally in the $\pm X$ direction in phase with $\ddot{X}(t)$. This drove oscillations in the X mode but not in the

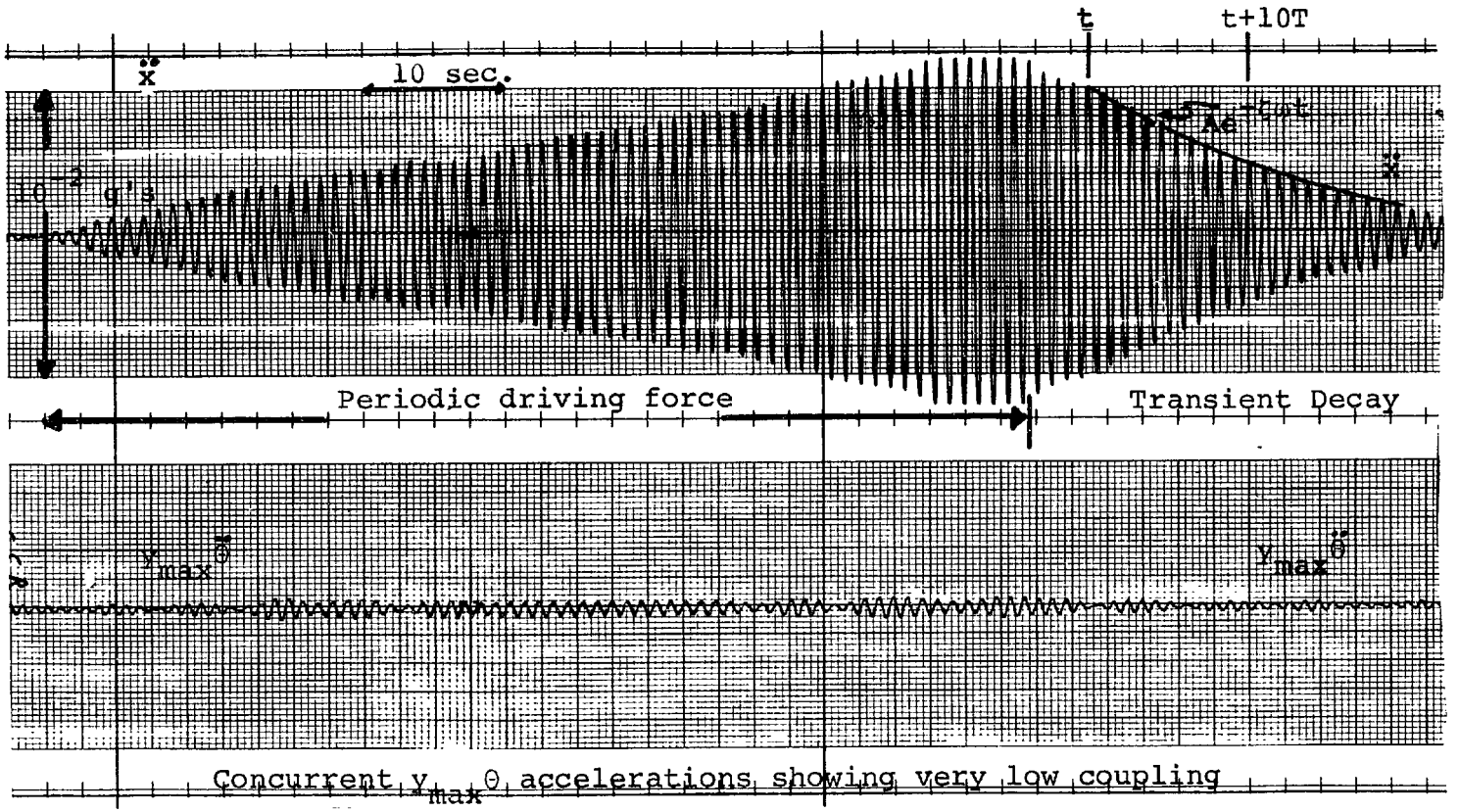

Figure IX-1 Transient Decay of x Mode and Coupling Between x and θ Modes

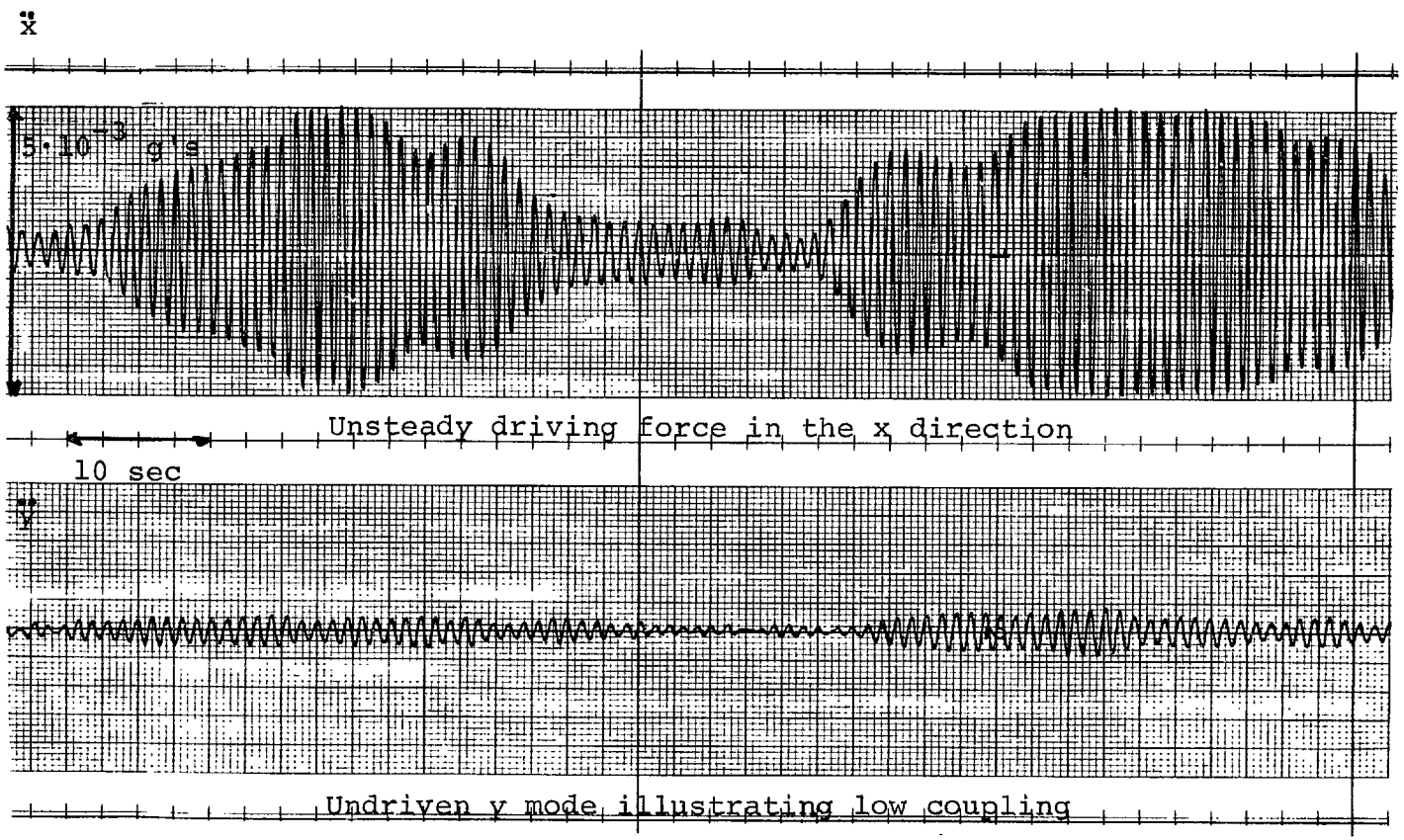

Figure IX-2 Coupling Between Artificially Excited x Mode and Undriven y Mode

Y or θ. The bottom half of Figure IX-1 shows the acceleration $Y_{max}\ddot{\theta}$, generated at the maximum Y coordinate of the structure by the $\ddot{\theta}$ angular accelerations. This motion resulted from coupling between the X and θ modes. Similarly, Figure IX-2 shows the coupling between the X and Y modes when only the X mode is driven. The amplitudes of the coupled motions are about 5% and 10% for the θ and Y modes, respectively. Since the average energy is proportional to the square of the measured accelerations, then the coupled modes have less than 1% of the energy of the driven modes. This is a substantiation of the assumption of negligible coupling between modes, which led to the choice of the independent single d.o.f. model.

X. PREDICTED RESPONSE OF THE BUZZARDS BAY LIGHT STATION TO WIND EXCITATION

To estimate the response of the tower to wind excitation using Equation VIII-10, it is necessary to know the wind force spectrum $S_F(\omega)$. There is not an abundance of information on wind force spectra. The most commonly cited authority is Alan G. Davenport [12]. He has proposed that the spectrum of the turbulent pressure fluctuations on large objects (typically buildings) can be represented by:

$$S_p(f) = 4P_1^2 J_z^2 J_H^2 \frac{S_v(f)}{V_1^2} \qquad (X\text{-}1)$$

where $P_1 = \frac{1}{2}\rho V_1^2 C_p$, the mean maximum pressure on the object. This is usually near the top of the structure where V_1, the mean wind speed is the highest. The highest pressure is the stagnation pressure for which $C_p = 1.0$. J_z and J_H are reduction factors that are less than or equal to one and depend on the geometry of the structure. $S_v(f)$ is the velocity spectra of the turbulent wind fluctuations, and f is the frequency in Hz.

$$S_v(f) = \frac{4C_T V_1^2}{f} \frac{x^2}{(1 + x^2)^{4/3}} \left[\frac{ft^2}{sec^2} - sec\right] \qquad (X\text{-}2)$$

where: C_T = terrain roughness coefficient equal to 0.001 for ocean and near coastal regions

$x = 4000\ f/V_{33}$

V_{33} = mean wind speed at 33 feet above ground

For $f \simeq 1$ Hz and $V_{33} \leq 200$ ft/sec, $x^2 >> 1$ and Equation X-2 simplifies to:

$$S_v(f) = \frac{4C_T V_1^2}{f} \left(\frac{V_{33}}{4000f}\right)^{2/3} \qquad (X-3)$$

V_{33} is related to V_1 by the equation:

$$\left(\frac{V_z}{V_{z_o}}\right) = \left(\frac{z}{z_o}\right)^{1/7.5} \qquad (X-4)$$

z and z_o are two different heights above ground, and V_z, V_{z_o} are corresponding velocities. For the BBT, $V_1 = V_{84}$, the velocity 84 feet above the sea surface. Therefore $V_{33} = 0.88V_1$ and $V_{33}/4000f = V_1/4530f$. Substituting this result and the value $C_T = 0.001$ into Equation X-3 reveals that:

$$S_v(f) = 1.461 \times 10^{-5} \left(\frac{V_1^{8/3}}{f^{5/3}}\right) \qquad (X-5)$$

The force spectrum can be related to the pressure spectrum by the frontal area A over which the pressure acts. $A \simeq 2000$ ft^2 for the BBT.

$$S_F(f) = A^2 S_p(f) \qquad (X-6)$$

Combining Equations X-1, X-5, and X-6 results in:

$$S_F(f) = 4A^2(\tfrac{1}{2}\rho C_p V_1^2)^2 \frac{J_z^2 J_H^2}{V_1^2} \left[1.461 \cdot 10^{-5} \frac{V_1^{8/3}}{f^{5/3}}\right] \qquad (X-7)$$

which reduces when $\rho_{air} = 0.00238$ slugs/ft^3, $C_p = 1.0$, and

A = 2000 ft^2 to:

$$S_F(f) = 3.310 \cdot 10^{-4} J_z^2 J_H^2 \frac{V_1^{14/3}}{f^{5/3}} \qquad (X\text{-}8)$$

Davenport suggests[12] that:

$$J_z^2 = \frac{1}{(1+\alpha)^2} \cdot \frac{1}{(1+\frac{C}{3})} \qquad (X\text{-}9a)$$

$$J_H^2 = \frac{1}{(1+\frac{C^1}{2})} \qquad (X\text{-}9b)$$

where: $\alpha = 0.16$

$C = 8hf/V_1 = 144 \frac{f}{V_1}$

h = 18 ft, height of house on top of tower

$C^1 = 20bf/V_1 = 1500 \frac{f}{V_1}$

b = 75ft, length of house

Substitution into Equation X-8 yields:

$$S_F(f) = \frac{2.46 \cdot 10^{-4} V_1^{14/3}}{f^{5/3}(1+\frac{144f}{V_1})(1+\frac{1500f}{V_1})} \qquad (X\text{-}10)$$

Recalling Eq. VIII-10 and noting that $S_F(\omega) = \frac{1}{2\pi} S_F(f)$, then

$$\langle E \rangle = \frac{\pi}{4} \frac{S_F(\omega_o)}{\zeta \omega_o M} = \frac{S_F(f_o)}{16 \pi \zeta f_o M} \qquad (X\text{-}11)$$

This is the expression for the average energy for any particular

mode with natural frequency f_o, driven by a wind force with spectrum $S_F(f_o)$ evaluated at f_o. For the BBT f_o = 0.975 Hz for the X and Y modes. The mean energy for the flexure modes was computed and plotted in Figure X-1, as a function of wind speed, for M = 18.7 x 10^3 slugs, ζ = 0.01. For example, for V_1 = 84.5 ft/sec = 50 kts:

$$\langle E \rangle_{x,y} = 0.51 \quad \text{ft-lbs} \tag{X-12}$$

These results as shown in Fig. X-1 are relatively crude. The expressions used for J_z^2 and J_H^2 were empirically derived for buildings and do not necessarily extend accurately to BBT-type structures. Of course, the expression for $S_p(f)$ has numerous inherent assumptions and approximations as well. Nonetheless, as will be shown in Section XII; the predictions agree quite well with measured results.

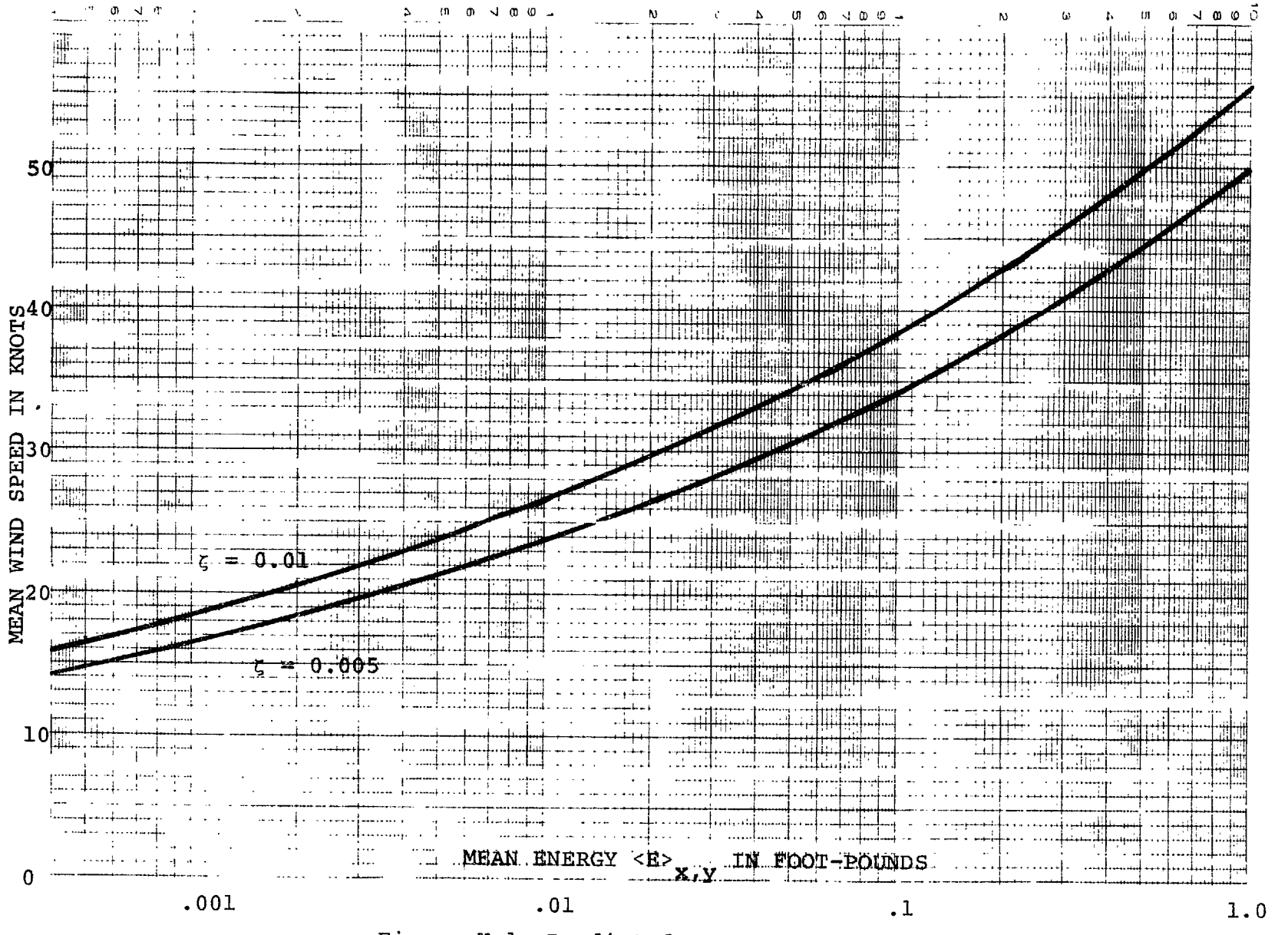

Figure X-1 Predicted Mean Energy per Mode vs Wind Speed for the Buzzards Bay Tower

XI. STATISTICAL ENERGY ANALYSIS PREDICTION OF STRUCTURAL RESPONSE TO WAVE EXCITATION

A. Application of SEA to the Ocean

The origin of Statistical Energy Analysis can be traced back fifteen years to the work of R.H. Lyon and P.W. Smith[15]. Working first independently and then jointly, they discovered that "... the response of a resonator excited by a diffuse broad band sound field, reached a limit when the radiation damping of the resonator exceeded its internal damping..," and furthermore "this limiting vibration amounted to an equality of energy between the resonator and the average modal energy of the sound field."[15]. In recent years these principles have been developed extensively for the interaction of sound and structural vibration. The similarity between the wave description of a sound field and the wave description of the surface of the ocean leads one to believe that the principles of SEA can be extended to the ocean. It can be shown that the behavior of a mechanical resonator driven by random ocean waves can be described in the same way as its acoustic analogy. The above two quotations, taken from Lyon's text on SEA, provide the two approaches that will arrive at the correct conclusions.

The first statement suggests that, by examining the relationship between damping and response of a resonator to random ocean waves, a limiting vibration can be calculated.

The alternate approach suggested by the second statement is

that if a quantity analogous to "the average modal energy of the sound field" can be determined for the ocean, then this will be the limit of maximum energy that a resonator can achieve in the ocean. By using a simple model of the ocean, an expression for the average modal energy will be derived. By a more fundamental approach the response of a resonator to random ocean waves will be shown to equal "average modal energy" in the limit of dominant radiation damping. Furthermore, this result will yield the resonant energy for non-limiting cases as well.

B. Average Modal Energy

To compute the average energy per mode for a random sea, expressions are required for the average energy over a frequency band $\Delta\omega$ and also the average number of modes contained in the same band. The average energy per unit area associated with a single ocean wave is given by:[16]

$$E = \tfrac{1}{2}\rho g A^2 \qquad (XI-1)$$

where: $\eta(x,t) = A\cos(kx-\omega t)$ The free surface equation

ρ = density of water

g = acceleration of gravity

This can be generalized to the energy spectrum of a random sea.

$$E(\omega) = \rho g S_{\eta}(\omega) \qquad \text{energy per unit frequency per unit area} \qquad (XI-2)$$

where: $S_{\eta}(\omega)$ = wave height spectrum

Over a frequency band $\Delta\omega$ the average energy per unit area is simply:

$$E(\omega)\,\Delta\omega \tag{XI-3}$$

Consider an infinitely deep ocean of length ℓ_1 and width ℓ_2, as shown in Figure XI-1. A solution to the boundary value problem for the velocity potential is as follows:

$$\phi(x_1, x_2, z, t) = \frac{gA}{\omega} e^{Kz} \cos k_1 x_1 \cos k_2 x_2 \cos \omega t \tag{XI-4}$$

In addition to satisfying the zero velocity boundary conditions on the walls, and at $z = -\infty$, it must satisfy:

$$\nabla^2\phi = 0$$

which is true if:

$$K^2 = k_1^2 + k_2^2 = \left(\frac{n_1\pi}{\ell_1}\right)^2 + \left(\frac{n_2\pi}{\ell_2}\right)^2 \equiv K_{n_1,n_2}^2 \tag{XI-5}$$

and must also satisfy:

$$\frac{\partial^2\phi}{\partial t^2} + g\frac{\partial\phi}{\partial z} = 0 \quad \text{on } z = 0 \tag{XI-6}$$

which results in $K = \omega^2/g$.

A convenient way[15] of ordering the modes K_{n_1, n_2} is shown in Figure X-2. Each point in this wave number lattice corresponds

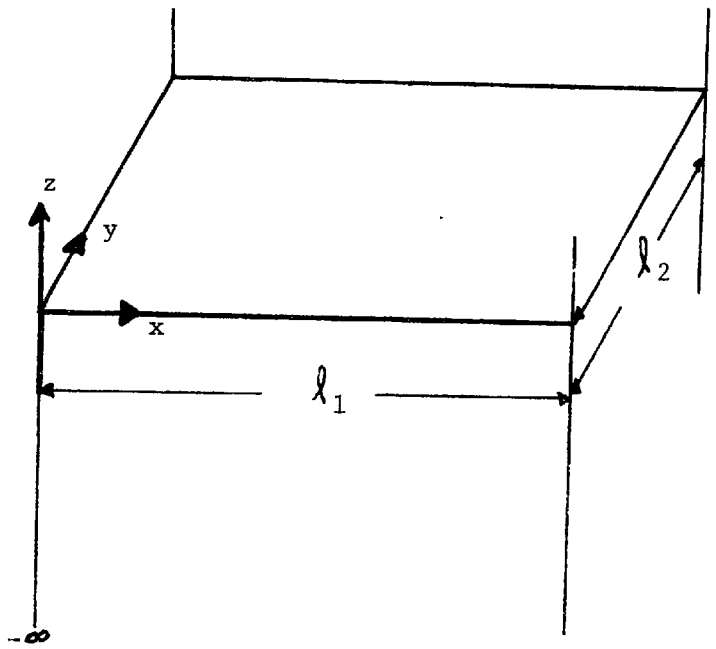

Figure XI - 1 Rectangular, Infinitely Deep Ocean

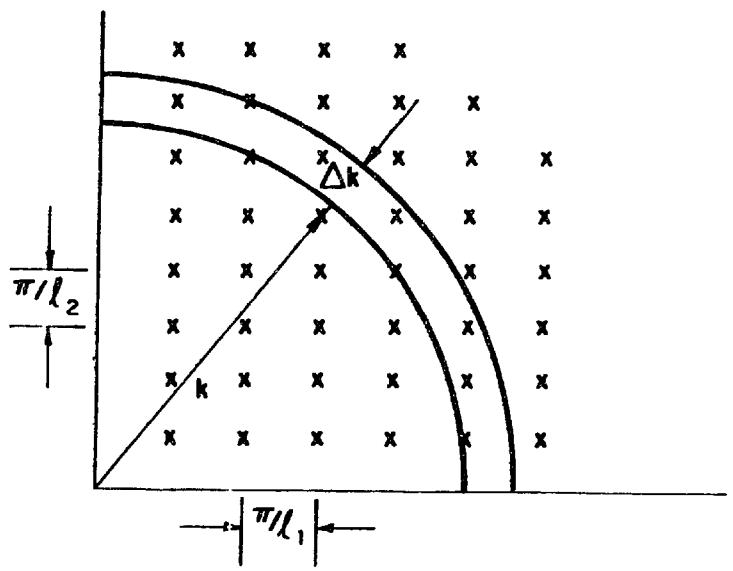

Figure XI - 2 Wave Number Lattice

to an area $\Delta A_K = \pi^2/\ell_1\ell_2$. If the wave number is increased from K to K + ΔK, the area is increased by $\frac{1}{2}\pi K\Delta K$ and on the average this will include $\frac{1}{2}\pi K\Delta K/(\pi^2/\ell_1\ell_2)$ new modes. Therefore the average number of modes per unit increment in wave number is:

$$n(K) = \frac{K\ell_1\ell_2}{2\pi} \qquad \text{(XI-7)}$$

which is called the modal density in wave number.

To obtain $n(\omega)$ the modal density in frequency, the relation $n(K)\Delta K = n(\omega)\Delta\omega$ is required. Using this and Eq. XI-7:

$$n(\omega) = n(K)\frac{\Delta K}{\Delta\omega} = \frac{K\ell_1\ell_2}{2\pi}\frac{\Delta K}{\Delta\omega} = \frac{K\ell_1\ell_2}{2\pi C_g} \qquad \text{(XI-8)}$$

Where we used the fact that $\frac{d\omega}{dk} = C_g$, the group velocity, which is one half the phase velocity C_ϕ for deep water waves. Since $K = \omega/C_\phi$, then:

$$n(\omega) = \frac{\omega\ell_1\ell_2}{\pi C_\phi^2} \left\{ \frac{\text{modes}}{\text{unit freq}} \right\} \qquad \text{(XI-9)}$$

The number of modes in a band $\Delta\omega$ is simply $n(\omega)\Delta\omega$, and by recalling Equation XI-3 and noting that $\ell_1\ell_2$ is the area of the rectangular ocean, then the average energy in a band $\Delta\omega$ for an area $\ell_1\ell_2$ is:

$$E(\omega)\Delta\omega\ell_1\ell_2 \qquad \text{(XI-10)}$$

and the average energy per mode is given by:

$$\langle E \rangle_{mode} = \frac{E(\omega)\Delta\omega\, \ell_1 \ell_2}{n(\omega)\,\Delta\omega} = \frac{E(\omega)\,\ell_1 \ell_2\, \pi C_\phi^2}{\omega \ell_1 \ell_2}$$

$$= \frac{\pi C_\phi^2 E(\omega)}{\omega} = \frac{\pi g^2}{\omega^3} E(\omega) \qquad (XI-11)$$

Substituting in for $E(\omega)$ from Eq. XI-2:

$$\langle E \rangle_{mode} = \pi\rho \frac{g^3}{\omega^3} S_\eta(\omega) \qquad (XI-12)$$

This is the average modal energy we set out to find.

One might argue that the rectangular ocean model is too artificial. It should be noted, however, that the geometry of the ocean does not enter into the final expression and that, as will be shown, the same result will be obtained by examining the response of a resonator to random waves. That is, the maximum energy a mechanical resonator in the ocean may have is given by Eq. XI-12, when evaluated at $\omega = \omega_0$, the natural frequency of the resonator. This maximum is achieved when the radiation damping is much larger than the internal damping.

C. Response of a Resonator to Sinusoidal Waves

The dynamic response of a complex structure to ocean waves can be thought of as the superposition of many individual natural modes. As in the case of the Buzzards Bay Tower, it is often possible to igrore the small coupling between modes and consider each mode independently, treating it analytically as if it were a single degree of freedom resonator.

The general formulation for one such independent resonator might be specified as follows:

$$M\ddot{x} + (R_i + R_r)\dot{x} + Kx = Fe^{i(\omega t + \phi)} \qquad \text{(XI-13)}$$

All of the constants and variables indicated above are the single d.o.f. equivalents to their modal counterparts. The mass includes the added mass of entrained fluid, and the spring constant includes both mechanical and hydrostatic effects. The damping coefficient is separated into two parts. R_r is called the radiation resistance and accounts for the dissipation of power by radiation of waves. The internal resistance R_i accounts for all other sources, such as viscous effects and soils dissipation. F is the magnitude of the "blocked force" an incident wave would exert on the resonator if it were held fixed.

In the next few pages an expression will be derived for the average energy of a resonator on the surface of the ocean in response to random waves. This average energy will be the product of the average energy per mode in the ocean, Eq. XI-12, and the ratio of the radiation damping to the total damping coefficient. This derivation draws heavily on similar work by

P. Smith[19] for the case of structural response to acoustic excitation.

Fundamental to these arguments is the principle of reciprocity. A more detailed discussion of reciprocity than that offered here may be found in the Smith reference[19]. Reciprocity is used to extend the known solution for the response of a certain class of resonators, floating ellipsoids, to the general case of an arbitrary resonator on the surface.

In general the blocked force exerted by the passage of the wave, $\eta e^{i\omega t}$, will be a function of frequency ω and angle of incidence Ω. To deal with this dependence on frequency and incidence angle, the "shape function" $\Gamma(\omega, \Omega)$ is defined as the ratio of the magnitude of the blocked force to the magnitude of the wave height. The abbreviated form will generally be used

$$F/\eta = \Gamma(\omega, \Omega) = \Gamma \qquad (XI\text{-}14)$$

in the following discussion. Consider two cases:

Case 1. An ellipsoid buoy, ballasted to float half submerged, is artificially driven at a sinusoidal velocity of magnitude V_b. The waves generated by this motion, in an otherwise calm deep ocean, are of height η_t in the vicinity of a second resonator, which is a large distance s from the buoy. The waves drive this resonator in steady state oscillation. For the sake of a name, this resonator represents one mode of an offshore tower. Henceforth variables subscripted t and b refer to the tower and buoy, respectively.

Case 2. The tower is driven sinusoidally with a magnitude V_t', where the prime now indicates the new problem represented as Case 2. The waves generated by this motion in an otherwise calm ocean are of height η_b' when they reach the buoy, which responds in steady state oscillation. The principle of point to point reciprocity in the fluid requires that:

$$\frac{|F_t|^2}{|V_b|^2} = \frac{|F_b'|^2}{|V_t'|^2} \qquad \text{(XI-15)}$$

In words, a buoy velocity V_b in Case 1 resulted in a blocked force F_t on the tower. The ratio of F_t to V_b must equal the ratio in the reverse Case 2 where a tower velocity V_t' resulted in a blocked force on the buoy F_b'.

One conclusion drawn from reciprocity is that the variation with angle of the radiated wave height is identical to the angular variation in blocked force due to waves of constant height but varying incidence angle. This angular dependence is accounted for mathematically by the directivity function $D(\Omega)$.

$$D(\Omega) = \frac{|\Gamma(\omega, \Omega)|^2}{\langle |\Gamma(\omega, \Omega)|^2 \rangle_\Omega} \qquad \text{(XI-16)}$$

Close examination of the two hypothetical cases described above, and application of the principle of reciprocity will yield an expression for the radiation resistance $R_{r,t}$ for the tower. This radiation resistance will be used to develop the desired expression for the modal energy of the tower due to random waves.

The power radiated by the buoy in Case 1, is given by the product of the mean square velocity and the radiation resistance. For oscillations of magnitude V_b,

$$\Pi_b = \tfrac{1}{2} |V_b|^2 R_r \qquad \text{(XI-17)}$$

The flux or intensity per linear foot along a circumference at a large radius s is given for plane waves by:

$$I_b = \frac{\tfrac{1}{4}\rho g^2 \eta_t^2}{\omega} = \frac{\tfrac{1}{2}|V_b|^2 R_{r,b}}{2\pi s} \qquad \text{(XI-18)}$$

Using the relation from XI-14, $\eta_t = F_t / \Gamma_t$, XI-18 can be rearranged to read:

$$\frac{|F_t|^2}{|V_b|^2} = \frac{\omega R_{r,b} |\Gamma_t|^2}{\pi s \rho g^2} D(\Omega)_b \qquad \text{(XI-19)}$$

The reciprocal expression for Case 2 can be written by inspection.

$$\frac{|F_b'|^2}{|V_t'|^2} = \frac{\omega R_{r,t} |\Gamma_b|^2 D(\Omega)_t}{\pi s \rho g^2} \qquad \text{(XI-20)}$$

J.N. Newman has shown[17] that for an ellipsoid on the surface:

$$F_b' = - \frac{4i\rho g \eta_b' P(\Omega)_b}{\omega} \qquad \text{(XI-21)}$$

and therefore:

$$\frac{|F_b'|}{|\eta_b'|} = \frac{4\rho g\,|P(\Omega)_b|}{\omega} = |\Gamma_b| \qquad \text{(XI-22)}$$

Newman has also shown that:

$$R_{r,b} = \frac{8\rho\omega}{g} < |P(\Omega)_b|^2 >_\Omega = \frac{\omega^3}{2\rho g^3} <|\Gamma_b|^2>_\Omega \qquad \text{(XI-23)}$$

where $< >_\Omega$ denotes the average over all angles. For bodies with a vertical axis of symmetry this can be reduced to:

$$R_{r,b} = |\Gamma_b|^2 \frac{\omega^3}{2\rho g^3} \qquad \text{(XI-24)}$$

This particular symmetry implies that F_b' and η_t are independent of angle from the buoy, and hence $D(\Omega)_b = 1$, and $|\Gamma_b|^2 = <|\Gamma_b|^2>_\Omega$.

To simplify the remainder of this discussion the result for the summetric case will be used. This implies no loss of generality, as the use of the general expressions will yield the same result. Equation XI-19 simplifies to:

$$\frac{|F_t|^2}{|V_b|^2} = \frac{\omega R_{r,b}\,|\Gamma_t|^2}{\pi s\rho g^2} \qquad \text{(XI-25)}$$

Substitution for $|\Gamma_b|^2$ from XI-24 into XI-20 yields:

$$\frac{|F_b'|^2}{|V_t'|^2} = R_{r,t}R_{r,b}D(\Omega)_t \frac{2g}{\pi s\omega^2} \qquad \text{(XI-26)}$$

Reciprocity requires that XI-25 equal XI-26 which leads to:

$$R_{r,t} = \frac{|\Gamma_t|^2}{D(\Omega)_t} \frac{\omega^3}{2\rho g^3} = \frac{\omega^3 <|\Gamma_t|^2>_\Omega}{2\rho g^3} \qquad \text{(XI-27)}$$

This is identical in form to the general expression given for $R_{r,b}$ in XI-23. Reciprocity has been used to show that the radiation damping coefficient of any resonator on the surface of the ocean is given by Eq. XI-27.

D. Response to Random Waves

The shape function expression for random waves is given by:

$$S_F(\omega) = |\Gamma(\omega, \Omega)|^2 S_\eta(\omega) \qquad \text{(XI-28)}$$

From Eq. VIII-10 the energy of a resonator excited by a broadband force spectrum is given by:

$$<E> = ME[\dot{x}^2] = \frac{\pi S_F}{2R_t} \qquad \text{(XI-29)}$$

where R_t is the total damping. In terms of Eq. XI-27 and XI-28, the average energy can be expressed by:

$$<E> = \frac{\pi S_\eta |\Gamma_t|^2}{2\left[R_i + \frac{\omega^3 <|\Gamma_t|^2>}{2\rho g^3}\right]} \qquad \text{(XI-30)}$$

$$= \frac{\pi \rho g^3}{\omega^3} S_\eta(\omega) \left[\frac{R_{r,t}}{R_{i,t} + R_{r,t}}\right] D(\Omega)_t$$

For waves of random incidence angle the average directivity function must be used, but it is always equal to 1.0 and XI-30 becomes:

$$\langle E \rangle = \frac{\pi \rho g^3}{\omega^3} S_\eta(\omega) \left[\frac{R_{r,t}}{R_{i,t} + R_{r,t}}\right] \qquad \text{(XI-31)}$$

This is the result we set out to find. The average modal energy of the resonator is simply the product of the average energy per mode in the ocean and the ratio of the radiation to total damping. Furthermore, for the special case of axial symmetry $D(\Omega)_t = 1$ and the above expression holds for random waves of any specified directional nature.

As the radiation damping becomes large compared to the internal damping the limiting vibration energy is reached and is found to equal the average energy per mode in the wave field as predicted. The assumptions inherent to the expression given in XI-31 follow:

1. No significant coupling between modes,
2. The radiation damping, added mass, and wave height spectrum all vary slowly with frequency over the resonant bandwidth,
3. Linearized internal damping,
4. The resonator is assumed to be moving at zero average velocity through the water.
5. Linearized water wave theory for deep water waves.

The suggestion is frequently made, "Why not use SEA techniques to consider the wind excitation as well?" The wave description and hence the principle of reciprocity are fundamental to SEA. For SEA to be applicable, a resonant structural mode is assumed to be in energy equilibrium with a large number of modes in the free field, in this case the water wave field. The structural mode must be able to receive energy from waves and to radiate energy as waves. This condition is satisfied in the case of acoustic excitation, water wave excitation, and possibly seismic excitation, but not wind excitation.

When the radiation damping is large compared to the internal damping, the resonant mode radiates energy as fast as it receives it. The average resonant energy equals the average energy per mode in the wave field, and there is no net power flow. When there is significant internal damping, the power dissipated by it must come from the external excitation. Power flow between the resonator and the free field is proportional to the difference in energy between the resonator and the average energy per mode in the ocean. Power flows from high energy to low energy, and therefore the energy of the resonator is less than the free field modal energy in accordance with Eq. XI-31.

For resonators in the ocean, the usefulness of SEA is limited by the assumptions listed above and by the engineer's ability to estimate the ratio of the radiation to the total damping. For many floating structures the radiation damping may dominate, and the limiting result can be easily computed. In such cases the SEA approach is superior to the classical random

vibration approach because it eliminates the need to compute a force spectrum from a wave height spectrum, a calculation which necessarily involves the structural details of each resonator. For structures in which the internal damping is known to be significant, then the SEA prediction becomes more difficult, requiring estimates of the internal and radiation damping, thus reducing the advantage over classical random vibration solutions. The simplicity of the SEA result contrasted to the complexity of the wind response prediction is a good example of the advantages that SEA has over the more classical solutions.

In the next section the measured response of the Buzzards Bay Tower will be compared to the expression derived here and to the previously computed wind driven response.

XII. COMPARISON BETWEEN PREDICTED AND MEASURED RESPONSE OF THE BUZZARDS BAY TOWER

A. Experimental Techniques

The instrumentation and Fast Fourier Transform analysis have been previously described. From the computed power spectra for the accelerations of the tower in flexure and rotation, the mean square acceleration was evaluated and from Eq. VIII-8b the mean square velocity was obtained. The mean energy is given by $M E[\dot{x}^2]$, $M E[\dot{y}^2]$ or $I E[\dot{\theta}^2]$ for flexure or torsional modes. These expressions were used to calculate the energy of vibration of the tower from more than fifty independent recordings, taken in a variety of weather conditions.

The greatest difficulty was encountered attempting to relate this response to the excitation. It was not practical to measure wave height spectra at the tower, but a sensitive anemometer was available. At the time each recording was made the average wind speed and direction was recorded, as well as the estimated sea state, including average wave and swell height, period and direction.

B. Interpreting the Data

The three modes on the tower had equal average energy, independent of the direction of the wind and waves. This is due in part to the coupling between modes, which acts to cause the modes to have equal energy, and to the relatively broad angular distribution of the wind and wave force spectra at any given

time.

The data points plotted in Figures XII-1 and XII-2 are the mean energy of the flexural and rotational modes versus mean wind speed. The scatter has several sources; each point was computed from a record 200 seconds long, which is short enough to allow considerable temporal variation from one measurement to the next. The mean wind speed does not account for variations in fetch and duration which determine sea state, nor does it account for variations of wind and wave forces with angle of incidence.

At certain times, the wind was observed to drop rapidly, leaving relatively high seas. These points are indicated in the figures. For two such data points arrows are drawn to the position of points that were plotted from data collected only a few minutes earlier at much higher wind speeds. These observationswere very helpful in separating the proportion of vibrational energy due to wind or waves.

C. Predicted Energy Due to Wind Excitation

In Section X the predicted energy of the flexural modes due to random wind loads was given in Eq. X-11 for the BBT. Due to lack of information in the literature, it was not possible to derive a similar expression for the energy of the torsional mode. From Eq. X-11, the average energy due to wind excitation is given by:

$$\langle E \rangle_{x,\,y} = \frac{S_F(f_o)}{16\pi\,\zeta f_o M}$$

where $S_F(f_o)$ is calculated from Eq. X-10. $\langle E \rangle_{x,\,y}$ is plotted in Figure XII-1 for M = 18.7 x 10^3 slugs, f_o = 0.9765 Hz, and ζ = 0.01. From Section IX ζ was found to vary from 0.007 for low amplitudes of vibration to 0.011 for higher oscillation amplitudes over the range of data plotted here. The effect of lower damping at low wind speeds would be to move the lower portion of the predicted curve slightly to the right. Most of the data points plotted in Figure XII-1 indicate that the flexural modal energy of the tower exceeded the wind energy prediction as is expected due to the additional wave excitation.

D. Predicted Energy Due to Waves

Eq. XI-26 gives the SEA prediction for the average energy per mode of a damped resonator in the ocean.

$$\langle E \rangle_{x,\,y,\text{ or }\theta} = \frac{\rho\pi g^3}{\omega^3} S_\eta(\omega) \left(\frac{R_r}{R_i + R_r}\right)$$

It consists of the product of the average energy per mode in the wave field, and the ratio of radiation to total damping. For the BBT the total damping is known, and $S_\eta(\omega)$ can be estimated from the observed wind speeds.

For the purpose of this prediction $S_\eta(\omega)$ was computed from the Pierson-Moskowitz spectrum[18]

$$S_\eta(\omega) = (8.1 \cdot 10^{-3}) \frac{g^2}{\omega^5} e^{-0.74(g/V\omega)^4} \text{ ft}^2\text{-sec} \quad \text{(XII-1)}$$

where V is the mean velocity at 19 meters above the surface and

was computed from the observed wind data.

The Pierson-Moskowitz spectrum is used here, for example, primarily because it is well known. It must be pointed out that like the numerous other published spectra available, it was computed from wave height data that was sampled at intervals greater that the periods of oscillation that we are interested in. The digitization interval for the Pierson Moskowitz was 1.5 sec[18], and therefore, Eq. XII-1 relies on the accuracy of the extrapolation to higher frequencies.

The limiting energy of vibration occurs when the radiation damping dominates, and this limit is plotted in Figure XII-1 and XII-2 for f_o = 0.9765 Hz and 1.085 Hz, respectively. It is immediately apparent that this limiting energy is not achieved.

The few data points obtained that allowed separation of the wind and wave energies make it possible to estimate the apparent correct location of the wave energy prediction, and from this deduce the ratio of radiation to total damping. The apparent energy line is plotted in Figure XII-1 and the ratio of the apparent energy to the maximum possible energy for winds above 20 knots indicates that:

$$\frac{b_{rad}}{b_{rad} + R_{int}} = \frac{0.1}{0.9} = 0.11 = \frac{\zeta_{rad}}{\zeta_{rad} + \zeta_{int}}$$

Since $\zeta_{rad} + \zeta_{int} = \zeta_{total} = 0.010$, then $\zeta_{int} = 0.0089$ and $\zeta_{rad} = 0.0011$. The internal damping is roughly eight times greater than the radiation damping. The viscous damping of the air and water

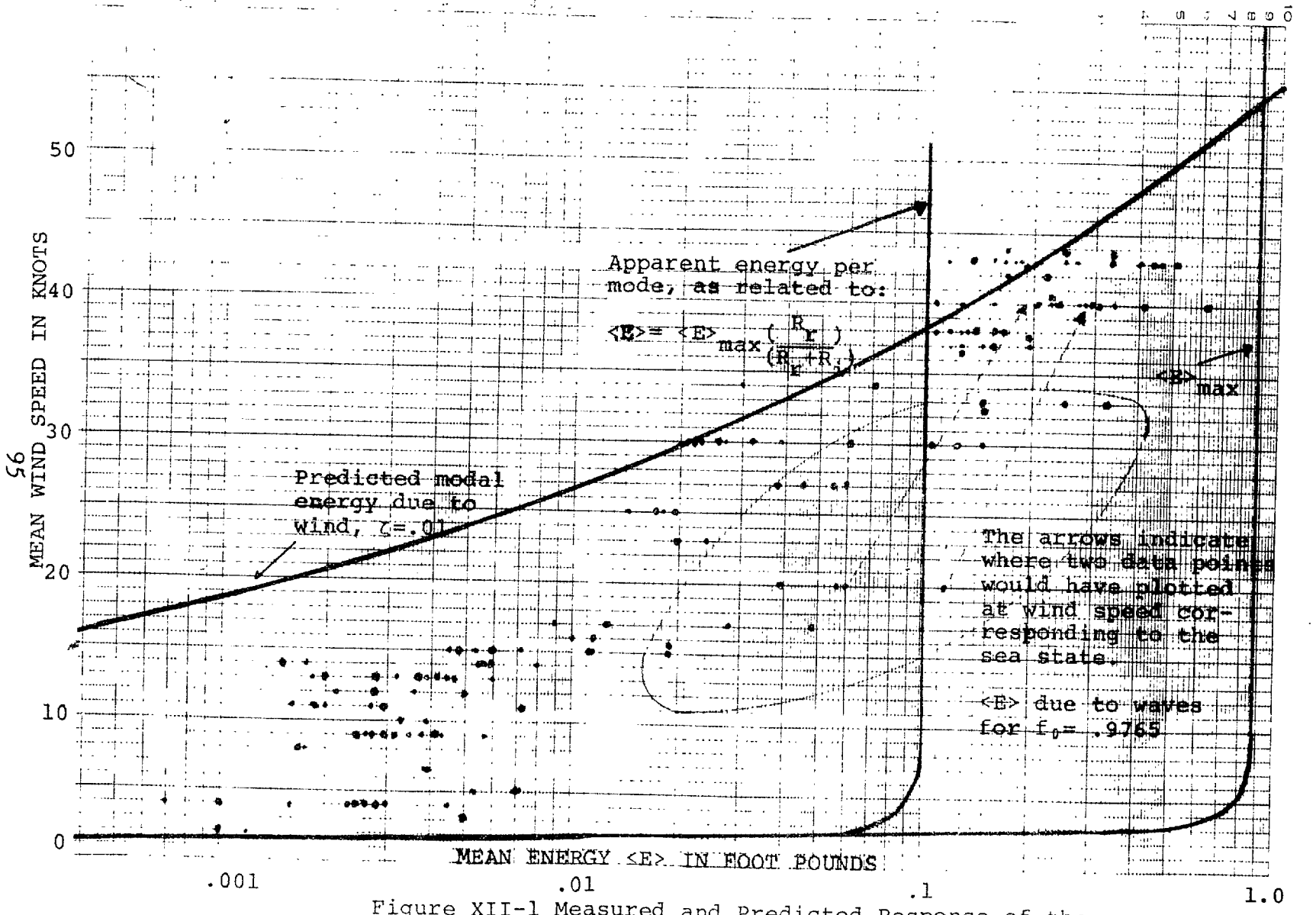

Figure XII-1 Measured and Predicted Response of the Buzzards Bay Tower Flexural Modes

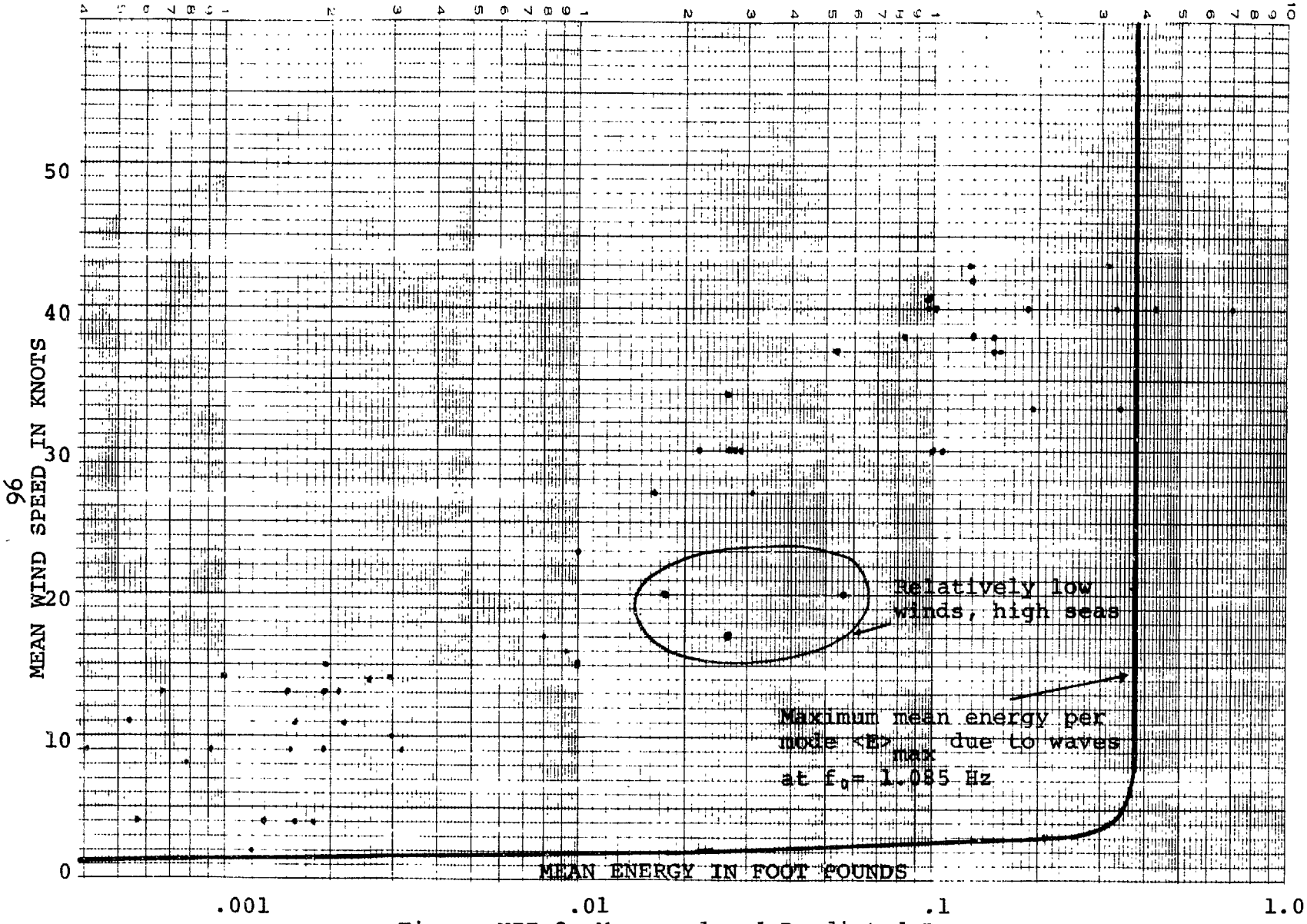

Figure XII-2 Measured and Predicted Response for the Torsional Mode

the strain damping in the structure, and the damping effect of the soil all combine to exceed the wave generating damping of the structure by several times. For winds below 20 knots the response cannot be accounted for completely by the predictions shown. A possible explanation is that at low wind speeds, the extrapolation from the Pierson-Moskowitz is in error, and yields high predictions for the vibrational energy due to waves..

E. Conclusion

The ability of the SEA model to predict a maximum response to waves has been confirmed for the case of the BBT. There are many unsolved vibration problems in the ocean, including buoy systems, floating ships and structures, as well as fixed towers. Statistical Energy Analysis is well suited to solving many of them. At the very least it can provide estimates of maximum response that can be of service to the designer of offshore systems. One of the next steps in the testing of the applicability of SEA might be to compare existing response measurements of offshore structures to the predictions of SEA.

REFERENCES

1. Tiedemann, H.M., Shortcomings of Offshore Subsurface Engineering Inspections, H.M. Tiedemann & Co., Inc., April 27, 1973.

2. ICES STRUDL II, The Structural Design Language, User's Manual, M.I.T. Press, Vol. 2, Second Edition, June, 1971.

3. Ackroyd, M.H., Whitman, R.V., A Review of Recent Mathematical Models Made on Actual Buildings and the Accuracy of Predicted Periods, NSF Grant GK-27955, Internal Study Report No. 33, May, 1973, Department of Civil Engineering, M.I.T., Cambridge, Massachusetts.

4. Vanmarcke, E.H., Iascone, R.N., Estimation of Dynamic Characteristics of Deep Ocean Tower Structures, Seagrant Report No. MITSG72-12, June 30, 1972, M.I.T.

5. Mansour, A.E., Millman, D.N., "Dynamic Random Analysis of Fixed Offshore Platforms", 1974 Offshore Technology Conference, Paper Number 2049.

6. Penzien, J., Kaul, M.K.,"Response of Offshore Towers to Strong Motion Earthquakes", Earthquake Engineering and Structural Dynamics, Vol. 1, pp. 55-68, 1972.

7. Berge, B., Penzien, J., "Three-Dimensional Stochastic Response of Offshore Towers to Wave Forces", 1974 Offshore Technology Conference, Paper Number 2050.

8. Vanstone, R.A., "Buzzards Bay Light Station Engineering Instrumentation Program", Brewer Engineering Laboratories Report 293, Marion, Massachusetts, 1964.

9. Reese, L.C., Cox, W.R., Koop, F.D., "Analysis of Laterally Loaded Piles in Sand", 1974 Offshore Technology Conference, Paper Number 2080.

10. Vandiver, J.K., "Oscillation Forces on Liquid-Filled Rectangular Tanks", unpublished manuscript, Harvey Mudd College, 1968.

11. Lumley, J.L., Panofsky, H.A., The Structure of Atmospheric Turbulence, Interscience Monographs and Texts in Physics & Astronomy, Vo. XII, John Wiley & Sons, New York, 1964.

12. Davenport, A.G., "Gust Loading Factors", Journal of the Structural Division, A.S.C.E., ST3, June, 1967, pp. 11-34.

REFERENCES, CONTINUED

13. Sachs, P., Wind Forces in Engineering, Monographs in Civil Engineering, Vol. 3, Pergamon Press, New York, 1972.

14. Crandall, S.H., Mark, W.D., Random Vibration in Mechanical Systems, Academic Press, New York, Fifth Edition, 1972.

15. Lyon, R.H., Statistical Energy Analysis for Designers, Parts I and II, Technical Report AFFDL-TR-74-56, Air Force Flight Dynamics Laboratory, Wright-Patterson A.F.B., Ohio.

16. Newman, J.N., Marine Hydrodynamics, Massachusetts Institute of Technology, Dept. of Ocean Engineering, Lecture Notes, 1971.

17. Newman, J.N., "The Exciting Forces on Fixed Bodies in Waves", Journal of Ship Research, Society of Naval Architects and Marine Engineers, Vol. 6, No. 3, December, 1962.

18. Neumann, G., Pierson, W.J., Principles of Physical Oceanography, Prentice-Hall, Inc., Englewood Cliffs, N.Y., 1966.

19. Smith, P., "Response and Radiation of Structural Modes Excited by Sound" Journal of the Acoustical Society of America, Vol. 34, No. 5, May 1962.

APPENDIX STRUDL COMPUTER MODEL

```
// 'KIM VANDIVER',CLASS=A,REGION=400K
/*MITID USER=(M11249,12334,,,TOWER)
/*SRI LOW
/*MAIN TIME=5,LINES=5
/*FORMAT PR,DDNAME=FT06F002
/*SETUP DDNAME=DUM,UNIT=2314,ID=(234065),A=FCM,                    X
/*COMM='USING M11113-4156'
//JOBLIB DD DSNAME=ICES.LINKLIB,DISP=SHR
// DD DSN=ICES.STRUDL.MODULES,DISP=SHR
// EXEC ICES,PROG=QQQICEX2
//GO.DD2 DD DSN=ICES.STRUDL.DATA,DISP=OLD
//GO.DD3 DD DSN=ICES.STRUDL.CDB,DISP=OLD
//GO.SYSIN DD *
STRUDL 'PLATFORM' 'STIFFNESS MATRIX FOR FULL TOWER'
DUMP TIME
UNITS LBS FEET
TYPE SPACE FRAME
JOINT COORDINATES
1 -.686 -10.0 30.686 S
2 60.686 -10.0 30.686 S
3 60.686 -10.0 -30.686 S
4 -.686 -10.0 -30.686 S
5 0.0 0.0 -30.0
6 0.0 0.0 0.0
7 0.0 0.0 30.0
8 30.0 0.0 30.0
9 60.0 0.0 30.0
10 60.0 0.0 0.0
11 60.0 0.0 -30.0
12 30.0 0.0 -30.0
13 57.5 36.5 -27.5 S
14 30.0 36.5 -27.5 S
15 2.5 36.5 -27.5 S
16 2.5 36.5 0.0 S
17 2.5 36.5 27.5 S
18 30.0 36.5 27.5 S
19 57.5 36.5 27.5 S
20 57.5 36.5 0.0 S
21 55.0 73.0 -25.0 S
22 30.0 73.0 -25.0 S
23 5.0 73.0 -25.0 S
24 5.0 73.0 0.0 S
25 5.0 73.0 25.0 S
26 30.0 73.0 25.0 S
27 55.0 73.0 25.0 S
28 55.0 73.0 0.0 S
29 55.0 102.0 -25.0
30 5.0 102.0 -25.0
31 5.0 102.0 25.0
32 55.0 102.0 25.0
33 55.0 117.0 -25.0
34 42.5 117.0 -25.0
35 30.0 117.0 -25.0
36 17.5 117.0 -25.0
37 5.0 117.0 -25.0
38 5.0 117.0 -12.5
39 5.0 117.0 0.0
40 5.0 117.0 12.5
41 5.0 117.0 25.0
```

```
42 17.5 117.0 25.0
43 30.0 117.0 25.0
44 42.5 117.0 25.0
45 55.0 117.0 25.0
46 55.0 117.0 12.5
47 55.0 117.0 0.0
48 55.0 117.0 -12.5
49 55.0 127.0 -25.0 S
50 30.0 127.0 -25.0 S
51 5.0 127.0 -25.0 S
52 5.0 127.0 0.0 S
53 5.0 127.0 25.0 S
54 30.0 127.0 25.0 S
55 55.0 127.0 25.0 S
56 55.0 127.0 0.0 S
57 -3.425 -50.0 33.425 S
58 63.425 -50.0 33.425 S
59 63.425 -50.0 -33.425 S
60 -3.425 -50.0 -33.425 S
MEMBER INCIDENCES
101 1 7
102 2 9
103 3 11
104 4 5
105 5 15
106 7 17
107 9 19
108 11 13
109 13 21
110 19 27
111 17 25
112 15 23
113 27 32
114 21 29
115 23 30
116 25 31
117 31 41
118 32 45
119 29 33
120 30 37
121 37 51
122 41 53
123 45 55
124 33 49
125 7 8
126 8 9
127 10 9
128 11 10
129 12 11
130 5 12
131 5 6
132 6 7
133 25 26
134 26 27
135 28 27
136 21 28
137 22 21
138 23 22
139 23 24
140 24 25
```

141 6 8
142 8 10
143 12 10
144 6 12
145 26 28
146 22 28
147 24 22
148 24 26
149 7 18
150 9 18
151 9 20
152 11 20
153 11 14
154 5 14
155 5 16
156 7 16
157 17 26
158 19 26
159 19 28
160 13 28
161 13 22
162 15 22
163 15 24
164 17 24
165 16 18
166 18 20
167 14 20
168 16 14
169 17 18
170 18 19
171 20 19
172 13 20
173 14 13
174 15 14
175 15 16
176 16 17
177 41 42
178 42 43
179 43 44
180 44 45
181 46 45
182 47 46
183 48 47
184 33 48
185 34 33
186 35 34
187 36 35
188 37 36
189 37 38
190 38 39
191 39 40
192 40 41
193 39 43
194 43 47
195 35 47
196 39 35
197 53 42
198 42 54
199 54 44
200 44 55

```
201 46 55
202 46 56
203 48 56
204 48 49
205 34 49
206 50 34
207 36 50
208 51 36
209 51 38
210 38 52
211 52 40
212 40 53
213 31 42
214 32 44
215 32 46
216 29 48
217 29 34
218 30 36
219 30 38
220 31 40
221 53 54
222 54 55
223 56 55
224 49 56
225 50 49
226 51 50
227 51 52
228 52 53
229 57 1
230 58 2
231 59 3
232 60 4
UNITS INCHES
CONSTANTS E 30000000. ALL
G 11500000. ALL
POISSON .333 ALL
UNITS KIPS
$ BOUNDARY CONDITIONS
$ 1 2 3 4 SPRING XZ SUPPORT ONLY
JOINT RELEASES FORCE Y MOMENT X Y Z KFX 30. KFZ 30.0
1 2 3 4
$ 57 58 59 60 MOMENT X Y Z KFX 200. KFZ 200. KFY  2000.
JOINT RELEASES MOMENT X Y Z KFX 200. KFY  2000. KFZ 200.
57 58 59 60
JOINT RELEASES FORCE X Y Z MOMENT X Y Z
13 TO 28 49 51 52 53 55 56
$ BOUNDARY CONDITIONS FOR UNIT DEFLECTION
JOINT RELEASES FORCE Y Z MOMENT X Y Z
50 54
$ 33 @ .500
MEMBER PROPERTIES PRISMATIC AX 51.1 IX 1.551E11 IY 6742. IZ 6742. SY 408.6 -
SZ 408.6
101 TO 112 229 230 231 232
$ 30 @ 1.00
MEM PROP PRI AX 91.2 IX 2.205E11 IY 9589. IZ 9589. SY 639.3 SZ 639.3
113 TO 124
$ 18 @ .500
MEM PROP PRI AX 27.49 IX 2.422E10 IY 1053.2 IZ 1053.2 SY 117. SZ 117.
149 TO 156
$ 18 @ .375
```

```
MEM PROP PRI AX 20.76 IX 1.855E10 IY 806.6 IZ 806.6 SY 89.63 SZ 89.63
169 TO 176
$ 16 ¢ .500
MEM PROP PRI AX 24.35 IX 1.684E10 IY 732. IZ 732. SY 91.5 SZ 91.5
157 TO 164
$ 16 ¢ .375
MEM PROP PRI AX 18.41 IX 1.293E10 IY 562.1 IZ 562.1 SY 70.3 SZ 70.3
125 TO 140
$ 14 ¢ .500
MEM PROP PRI AX 21.21 IX 1.113E10 IY 483.8 IZ 483.8 SY 69.1 SZ 69.1
177 TO 212
$ 12.75 ¢ .375
MEM PROP PRI AX 14.58 IX 6.425E9 IY 279.3 IZ 279.3 SY 43.82 SZ 43.82
213 TO 220
$ 10.75 ¢ .350
MEM PROP PRI AX 11.44 IX 3.560E9 IY 154.8 IZ 154.8 SY 28.8 SZ 28.8
141 TO 148
$ 8.625 ¢ .322
MEM PROP PRI AX 8.4 IX 1.668E9 IY 72.5 IZ 72.5 SY 16.81 SZ 16.81
165 TO 168
$ 24WF100 J = 4.87  IX = GJ
MEM PROP PRI AX 29.43 IX 5.6E7 IY 2987. IZ 203.5 SY 248.9 SZ 33.9
221 TO 228
LOADING 'UNIT 3' 'UNIT DEFLECTION IMPOSED AT Y = 127.0 IN +X DIRECTION'
JOINT DISPLACEMENT DISP X 1.0
50 54
LOADING 'TORSION' 'DETERMINE TORSIONAL RIGIDITY'
JOINT DISPLACEMENT DISP X -1.0
50
JOINT DISPLACEMENT DISP X 1.0
54
ACTIVE JOINTS ALL
ACTIVE MEMBERS ALL
ACTIVE LOADINGS ALL
UNITS INCHES KIPS
STIFFNESS ANALYSIS
PRINT APPLIED JOINT DISPLACEMENTS
LIST REACTIONS
$ ASYM BREAK ON COLUMN  126
ACTIVE JOINTS ALL
ACTIVE MEMBERS ALL BUT 126
ACTIVE LOADINGS ALL
STIFFNESS ANALYSIS
LIST REACTIONS
$ ASYM BREAK ON COLUMN  166
ACTIVE JOINTS ALL
ACTIVE MEMBERS ALL BUT 166
ACTIVE LOADINGS ALL
STIFFNESS ANALYSIS
LIST REACTIONS
$ ASYM BREAK ON COLUMN  142
ACTIVE JOINTS ALL
ACTIVE MEMBERS ALL BUT 142
ACTIVE LOADINGS ALL
STIFFNESS ANALYSIS
LIST REACTIONS
$ ASYM BREAK ON COLUMN  110
ACTIVE JOINTS ALL
ACTIVE MEMBERS ALL BUT 110
ACTIVE LOADINGS ALL
```

```
STIFFNESS ANALYSIS
LIST REACTIONS
$ ASYM BREAK ON COLUMN  145
ACTIVE JOINTS ALL
ACTIVE MEMBERS ALL BUT 145
ACTIVE LOADINGS ALL
STIFFNESS ANALYSIS
LIST REACTIONS
FINISH
/*EOJ ********
```

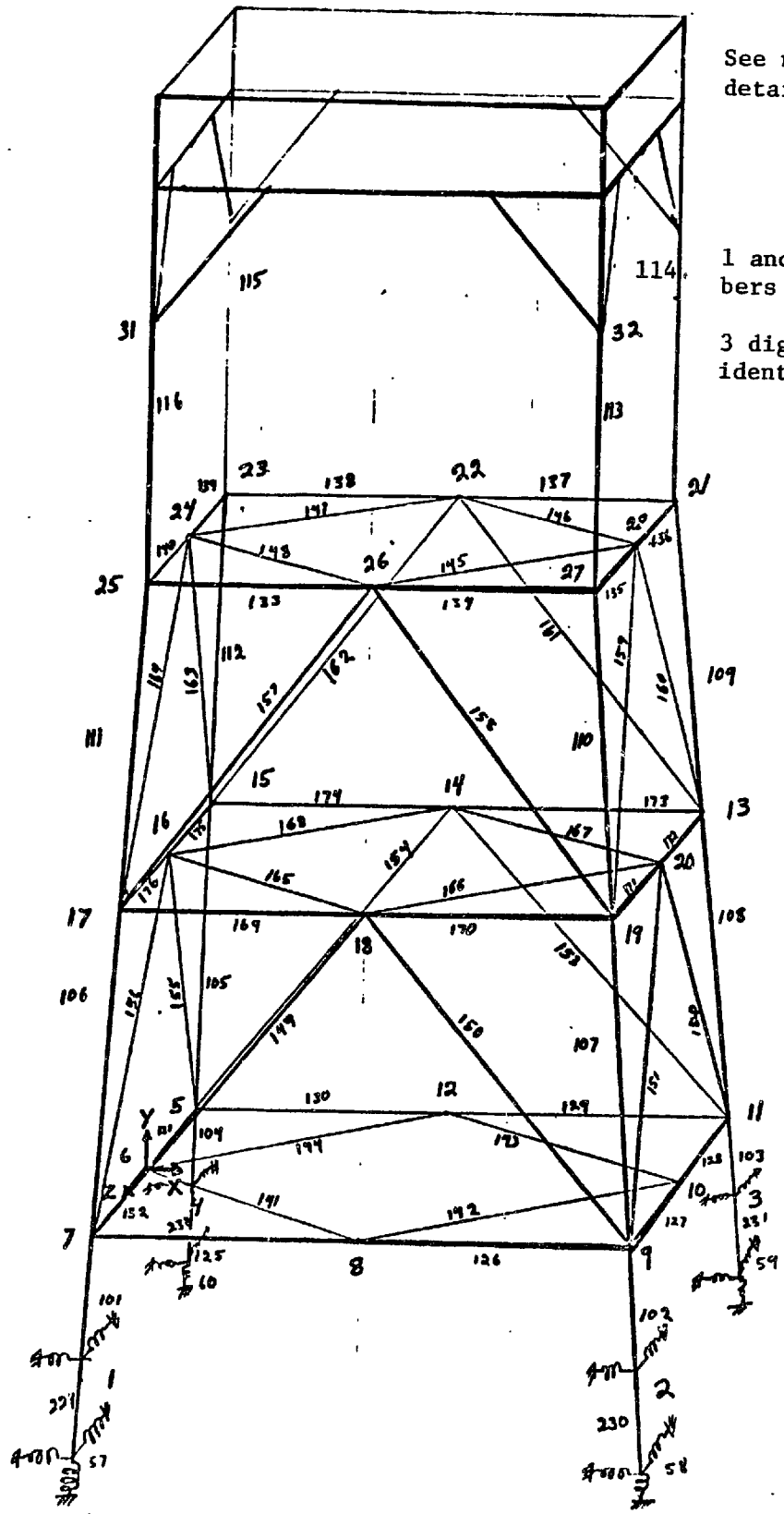

Appendix Figure I-A STRUDL Tower Model

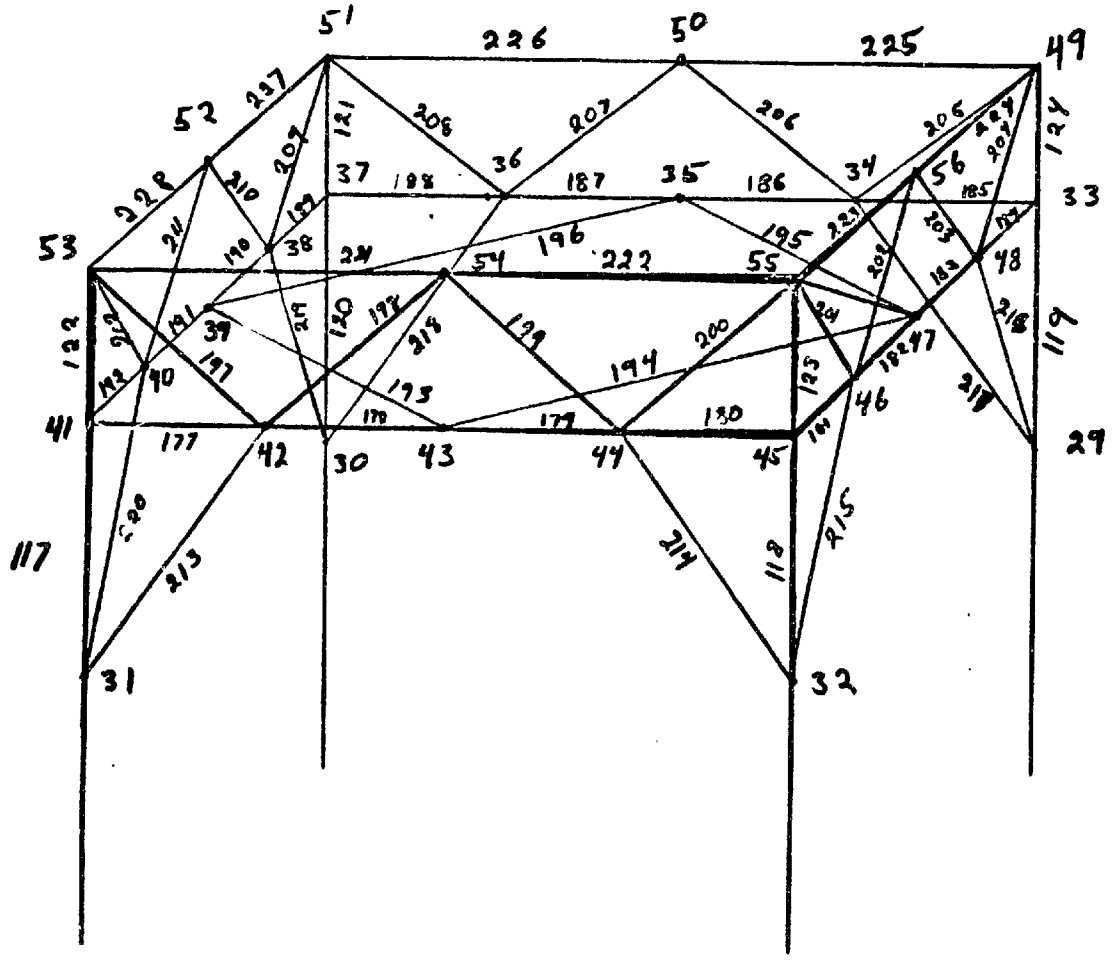

Appendix Figure I-B STRUDL Tower Top